MEASUREMENT OF FORMALDEHYDE DRY DEPOSITION AND AIR-WATER EXCHANGE WITH SURROGATE SURFACES

By

Remzi SEYFİOĞLU

September 2004

İZMİR

MEASUREMENT OF FORMALDEHYDE DRY DEPOSITION AND AIR-WATER EXCHANGE WITH SURROGATE SURFACES

A Thesis Submitted to the
Graduate School of Natural and Applied Sciences of
Dokuz Eylül University
In Partial Fulfillment of the Requirements for
the Degree of Doctor of Philosophy in Environmental Engineering, Environmental Technology Program

By
Remzi SEYFİOĞLU

September 2004
İZMİR

Ph.D. THESIS EXAMINATION RESULT FORM

We certify that we have read the thesis, entitled "MEASUREMENT OF FORMALDEHYDE DRY DEPOSITION AND AIR-WATER EXCHANGE WITH SURROGATE SURFACES" completed by M. Remzi SEYFİOĞLU under supervision of Assoc. Prof. Dr. Mustafa ODABAŞI and that in our opinion it is fully adequate, in scope and in quality, as a thesis for the degree of Doctor of Philosophy.

Assoc. Prof. Dr. Mustafa ODABAŞI

Supervisor

Prof. Dr. Gürdal TUNCEL

Jury Member

Prof. Dr. Aysen MÜEZZİNOĞLU

Jury Member

Assoc. Prof.Dr.Abdurrahman BAYRAM

Jury Member

Asst. Prof.Dr. Aysun SOFUOĞLU

Jury Member

Approved by the
Graduate School of Natural and Applied Sciences

Prof.Dr. Cahit HELVACI
Director

ACKNOWLEDGMENTS

I would like to express my gratitude to my advisor Assoc. Prof. Dr. Mustafa ODABAŞI for his invaluable advice, guidance and encouragement. Completion of this work would not have been possible without his help. I would like to thank Prof. Dr. Aysen MÜEZZİNOĞLU for her guidance, support and encouragement. I am also grateful to Assist. Prof. Dr. Aysun SOFUOĞLU for her review, comments and support.

I would like to present my deep appreciation to Assoc. Prof. Dr. Abdurrahman BAYRAM for his valuable support. I would like to express my appreciation to my colleagues Hulusi DEMİRCİOĞLU, Eylem ÇETİN, Sevde Seza BOZACIOĞLU, Hasan ALTIOK, Sinan YATKIN, and Yetkin DUMANOĞLU for their valuable help and support.

I would like to thank Dokuz Eylul University for financially supporting of my Ph.D. studies.

I would like to thank to my son Mert SEYFİOGLU and my daughter Cemre SEYFİOĞLU for their emotional support during my research.

M. Remzi SEYFİOĞLU

ABSTRACT

Concurrent dry deposition and ambient air samples were collected between May 2003 and May 2004 in Buca, İzmir. Dry deposition of formaldehyde was measured using a water surface sampler (WSS) and dry deposition plates. Wet deposition samples were also collected during this sampling period.

Average gas phase formaldehyde (HCHO) concentrations (7.3±6.5 μg m^{-3}, average± SD) were within the range previously measured at different sites around the world. Particle phase HCHO concentrations ranged between 3-65 ng m^{-3} (average±SD, 18±12 ng m^{-3}) and HCHO was primarily associated with gas-phase (99.55%).

Particle phase HCHO fluxes measured with dry deposition plates ranged between 2-56 μg m^{-2} day^{-1} (average±SD, 17±12 μg m^{-2} day^{-1}). Particulate phase dry deposition velocities calculated using the particulate fluxes measured with dry deposition plates and ambient particulate concentrations ranged from 0.1 to 9.6 cm s^{-1} (1.4±1.4 cm/s). The particulate overall dry deposition velocity agreed well with those measured previously for other pollutants using the same method.

Formaldehyde concentration was measured in 27 rain samples collected at the sampling site ranged between 10-304 μg l^{-1}. The annual formaldehyde wet deposition was calculated as 30155 μg m^{-2} yr^{-1}. The annual HCHO total deposition (wet+dry) was dominated by wet deposition (83.2%).

The range for gas phase HCHO flux was 273-5404 μg m^{-2} day^{-1} (1200±888 μg m^{-2} day^{-1}). The average total (gas+particle) flux measured with the WSS was dominated by gas phase flux (98.6%). The calculated gas-phase overall mass transfer coefficients

(K_g) ranged between 0.07-0.59 cm s^{-1} (0.25±0.12 cm s^{-1}). The K_g determined from laboratory experiments averaged as 0.60±0.22 cm s^{-1} and was 2.4 times higher than the average value calculated from field samples.

The measured K_g values in laboratory were compared to the predictions of two different models, one previously developed based on experiments performed with the WSS (for non-reactive species, considering no enhancement, Model I) and, one previously published (for reactive species, taking into account the enhancement due to chemical reaction, Model II). The results indicated that the Model I significantly underestimated the K_g while the predictions of Model II were in excellent agreement with those measured. Results indicated that under the laboratory conditions of this study, there was a flux enhancement of HCHO mass transfer due to chemical reaction and it ranged between 2.8 and 4.1 times.

For field studies, the average measured K_g (0.25 cm s^{-1}) was significantly lower than the average predictions of Model I (0.44 cm s^{-1}) and the Model II (0.90 cm s^{-1}). Since none of the proposed mechanisms (i.e., decreased deposition due to non-zero water concentration, sulfite/bisulfite interference, and loss due to chemical degradation or transformation) could fully explain the difference between the modeled and experimental K_g values, the difference was attributed to the propagated effect of these mechanisms.

Keywords: Dry deposition, formaldehyde, gas/particle partitioning, wet deposition, air-water exchange, deposition velocity, mass transfer coefficient, flux enhancement.

ÖZET

Kuru çökelme ve dış hava örnekleri eş zamanlı olarak Mayıs-2003 ve Mayıs-2004 tarihleri arasında Buca, İzmir'de toplanmıştır. Fromaldehit kuru çökelmesi su yüzeyi örnekleyicisi (WSS) ve kuru çökelme plakaları kullanarak ölçülmüştür. Bu örnekleme periyodunda ayrıca ıslak çökelme örnekleri de toplanmıştır.

Gaz fazdaki ortalama formaldehit (HCHO) konsantrasyonu (7.3±6.5 μg m^{-3}, ortalama±SD) daha önce değişik bölgelerde ölçülmüş değerler aralığındadır. Partikül faz HCHO konsantrasyonu 3 ile 65 ng m^{-3} (ortalama±SD, 18±12) aralığında değişmektedir ve atmosferik HCHO büyük oranda gaz fazdan oluşmaktadır (% 99.55).

Kuru çökelme plakalarıyla ölçülen partikül faz HCHO akısı, 2 ile 56 μg m^{-2} $gün^{-1}$ (ortalama±SD, 17±12 μg m^{-2} $gün^{-1}$) arasında ölçülmüştür. Partikül fazda kuru çökelme hızı, kuru çökelme plakalarında ölçülen, partikül akısı ve partikül fazdaki HCHO konsantrasyonu kullanılarak hesaplanmıştır ve fazda kuru çökelme hızı 0.1 ile 9.6 cm s^{-1} (1.4±1.4 cm/s) arasında değişmektedir. Partikül fazdaki kuru çökelme hızları, daha önce başka kirleticiler için aynı metod kullanılarak ölçülmüş hızlarla çok iyi uyuşmaktadır.

Toplanan 27 yağmur suyu örneğinde formaldehit konsantrasyonu 10-304 μg l^{-1} arasındadır. Yıllık formaldehid ıslak çökelmesi 30155 μg m^{-2} $gün^{-1}$ olarak hesaplanmıştır. Toplam HCHO (yaş+kuru) çökelmesinde, %83.2 oranla ıslak çökelme daha baskındır.

Gaz faz HCHO akısı 273-5404 µg m^{-2} $gün^{-1}$ (1200±888 µg m^{-2} $gün^{-1}$) aralığındadır. Su yüzeyi örneklemesi ile ölçülen toplam akıda (gaz+partikül) gaz faz akısı daha baskındır (%98.6). Gaz fazdaki kütle transfer katsayısı (K_g) 0.07-0.59 cm s^{-1} (0.25±0.12 cm s^{-1}) aralığında hesaplanmıştır. Laboratuvar çalışmalarında elde edilen K_g ortalama 0.60±0.22 cm s^{-1}'dir ve alan çalışmalarından elde edilen ortalama değerin 2.4 katıdır.

Laboratuvarda ölçülen K_g değerleri iki değişik model kullanılarak hesaplanan değerler ile karşılaştırılmıştır: Bir tanesi su yuzeyi örnekleyicisi kullanılan deneyleri baz alarak geliştirilmiş model (reaktif olmayan türler için, Model I), ve diğeri daha önce yayımlanmış model (reaktif türler için, kimyasal reaksiyonlardan dolayı kütle trasferinde artış olduğu kabul edilir, Model II). Sonuçlar göstermiştir ki Model I, K_g değerini önemli derecede beklenenden daha düşük belirlerken, Model II'nin tahminleri deneysel olarak ölçülenler ile mükemmel bir uyum içindedir. Sonuçlara göre, labratuvar koşulları altında, HCHO kütle transferinde kimyasal reaksiyonlardan dolayı akı artışı meydana gelmektedir ve bu akı artışı 2.8 ile 4.1 kat arasında değişmektedir.

Alan çalışmalarında ölçülen ortalama K_g değerleri (0.25 cm s^{-1}) Model I (0.44 cm s^{-1}) ve Model II (0.90 cm s^{-1})'nin ortalama tahminlerinden önemli derecede daha düşüktür. Öne sürülen mekanizmaların hiçbirisi (sıfır olmayan su konsantrasyonundan dolayı azalan çökelme, sülfit/bisülfit girişimi, kimyasal bozunma ya da dönüşümden dolayı kayıplar) model ve deneysel K_g değerleri arasındaki farkı tam anlamıyla açıklayamadığı için, meydana gelen fark bu mekanizmaların eklenik etkisine bağlanmıştır.

Anahtar sözcükler : Kuru çökelme, formaldehit, gaz/partikül fazları arasında dağılım, ıslak çökelme, hava-su arakesitinde madde taşınımı, çökelme hızı, kütle transfer katsayısı, akı artışı.

CONTENTS

Page

Chapter Three

Materials And Methods

Chapter Four

Results and Discussion

Chapter Five

Conclusions

LIST OF TABLES

LIST OF FIGURES

CHAPTER ONE
INTRODUCTION

Formaldehyde is a widely used chemical by industry to manufacture building materials and numerous household products. It is also emitted to the atmosphere as a result of incomplete combustion of fossil fuels. Vegetation and photochemical reactions are other identified sources of formaldehyde. Therefore, it is present in substantial concentrations in ambient air.

Formaldehyde, a colorless, pungent-smelling gas, can cause watery eyes, burning sensations in the eyes and throat, nausea, and difficulty in breathing in some humans exposed at elevated levels (above 0.1 ppm). High concentrations may trigger asthma attacks in people. It has also been shown to cause cancer in animals and may cause cancer in humans.

Following its release, formaldehyde is transported through the atmosphere where it is subject to chemical and physical transformations (Finlayson-Pitts and Pitts, 1986). Removal of formaldehyde from the atmosphere can occur by chemical transformations, rain and snow scavenging of vapors and particles, by dry deposition of particles, and by vapor exchange across the air-water interface (Bidleman, 1988). The most of the research on formaldehyde have been on precipitation monitoring, wet deposition and gas phase concentration measurements (Viskari et al., 2000; Khare et al., 1997; Anderson et al., 1995; Baez et al., 1994; Sakugawa and Kaplan, 1993). There are only a few studies on ambient particle phase concentrations (Klippel and Warneck, 1980; Deandrade et al.

1993; Deandrade et al. 1995; Liggio and McLaren, 2003) and air-water exchange (Zhou and Mopper, 1997).

Previous research indicated that the impact of atmospheric deposition of air pollutants to the surface waters is large (Hoff et al., 1996). However, there is no generally accepted method to directly measure or estimate dry deposition. The use of various types of surrogate surfaces is one approach that has been used to directly measure dry deposition. Recently, the water surface sampler (WSS) in conjunction with greased dry deposition plates has been successfully used to directly measure particle dry deposition and air-water exchange of organic and inorganic air pollutants which exist both in particulate and gas phases (Odabasi et al., 1999; Shahin et al., 1999; Cakan, 1999; Tasdemir, 1997; Yi et al., 1997).

Formaldehyde (HCHO) reacts substantially and reversibly with water to form methane diol (hydrated formaldehyde, $CH_2(OH)_2$). Formaldehyde occurs more than %99 as the diol when it is dissolved in water (Schwarzenbach et al., 1993). These reactions occur over time periods similar to those required for diffusive transfer across the water boundary layer resulting in a flux enhancement of formaldehyde. The flux enhancement of formaldehyde due to chemical reaction can be estimated using previously suggested models (Zhou and Mopper, 1997; Schwarzenbach et al., 1993; Schwarzenbach et al., 2003). However, it has not been determined experimentally.

The overall objective of this study was to quantify the flux enhancement of formaldehyde using the water surface sampler that has been used successfully as a research tool. The specific objectives were:

1. To measure directly particulate dry deposition and air-water exchange fluxes of formaldehyde using surrogate surfaces.

2. To determine the particulate phase dry deposition velocity and overall mass transfer coefficient for formaldehyde.

3. To evaluate the flux enhancement by comparing the experimental mass transfer coefficients of formaldehyde to the modeled ones.

4. To measure wet deposition of formaldehyde and to determine its relative importance in total (dry+wet) deposition.

5. To measure ambient particle and gas phase concentrations of formaldehyde and to investigate its gas/particle partitioning.

This study consists of five chapters. An overview and the objectives of the study were presented in Chapter 1. Chapter 2 reviews concepts and previous works related to this study. The details of experimental work were explained in Chapter 3. Results and discussions were presented in Chapter 4. Chapter 5 summarizes the conclusions and suggested future work.

CHAPTER TWO
LITERATURE REVIEW

This chapter presents background information on sources, ambient concentrations, dry and wet deposition, and air-water exchange of formaldehyde reported by different studies.

2.1. Sources of Formaldehyde

2.1.1 Natural sources

Formaldehyde occurs naturally in the environment and is the product of many natural processes. It is released during biomass combustion, such as forest and brush fires. In water, it is also formed by the irradiation of humic substances by sunlight (Kieber et al., 1990).

One of the sources of formaldehyde is known as the direct emission from biogenic sources. Kesselmeier et al., (1997), combined the measurement of monoterpene emissions with the simultaneous determination of the release rates of some oxygenated compounds, short-chained organic acids and aldehydes, from two typical Mediterranean tree species, a pine tree *(Pinus pinea)* and *Quercus ibex* and compared the observed emission with two algorithms, one for the release of isoprene and the other for monoterpenes. With this approach Kesselmeier et al., (1997), could get information about a direct release of the oxygenated compounds, acetic and formic acids, as well as, acetaldehyde and formaldehyde in comparison to the monoterpene emissions.

Furthermore, the emission data were used to calculate a carbon budget, comparing the assimilated carbon with the emitted carbon of monoterpenes, acids and aldehydes (Kesselmeier et al., 1997).

As a metabolic intermediate, formaldehyde is present at low levels in most living organisms. It is emitted by bacteria, algae, plankton, and vegetation (Nuccio et al., 1995).

2.1.2 Anthropogenic sources

Anthropogenic sources of formaldehyde include direct sources such as fuel combustion, industrial on-site uses, and off-gassing from building materials and consumer products.

On-road motor vehicles are the largest direct source of formaldehyde. Although formaldehyde is not present in gasoline, it is a product of incomplete combustion and is released, as a result, from internal combustion engines. The amount generated depends primarily on the composition of the fuel, the type of engine, the emission control applied, the operating temperature, and the age and state of maintenance of the vehicle (WEB_1, 2002).

Other anthropogenic combustion sources (covering a range of fuels from wood to plastics) include wood-burning stoves, fireplaces, furnaces, power plants, agricultural burns, waste incinerators, cigarette smoking, and the cooking of food (U.S. Consumer Product Safety Commission, 1997).

An amount in excess of billion pounds of a 37% aqueous solution of HCHO, known as formalin, is produced each year in North America (Ching et al., 1998). The solution is incorporated into urea-formaldehyde and phenol-formaldehyde resin, which are widely used in industry for the production of foam insulation, particle board and plywood.

These materials can emit formaldehyde in substantial amounts into the indoor environment.

2.1.3 Secondary formation

Carbonyls are among the major species of organic compounds involved in photochemical air pollution. Aldehydes and ketones have an important role as products of photo-oxidation of gas phase hydrocarbons and as a major source of free radicals. They are the most abundant of the easily photolyzed compounds in the atmosphere (Beaz et al., 1994).

Formaldehyde is formed in the troposphere by the photochemical oxidation of many types of organic compounds, including naturally occurring compounds, such as methane (US EPA, 1993) and isoprene (Tanner et al., 2001), and pollutants from mobile and stationary sources, such as alkanes, alkenes (e.g., ethene, propene), aldehydes (e.g., acetaldehyde, acrolein), and alcohols (e.g., allyl alcohol, methanol, ethanol) (Grosjean et al., 1996a, 1996b).

Important atmospheric trace gases such as methane (CH_4) and other hydrocarbons are mainly removed by OH radicals. Therefore the lifetime of these gases is determined by OH. The photochemical degradation of CH_4 yields formaldehyde:

$$CH_4 + OH \rightarrow CH_3 + H_2O \quad (2.1)$$

$$CH_3 + O_2 + M \rightarrow CH_3O_2 + M \quad (2.2)$$

$$CH_3O_2 + NO \rightarrow CH_3O + NO_2 \quad (2.3)$$

$$CH_3 + O_2 \rightarrow HCHO + HO_2 \quad (2.4)$$

Since this reaction sequence is strongly dependent on OH radicals, an influence of enhanced UV-B radiation is expected (WEB_2, 2002).

2.2. Ambient Concentrations

2.2.1. Gas phase concentrations

Given the diversity and abundance of formaldehyde precursors in urban air, secondary atmospheric formation frequently exceeds direct emissions from combustion sources, especially during photochemical air pollution episodes, and it may contribute up to 70–90% of the total atmospheric formaldehyde (WEB_1, 2002).

It was estimated that photochemical formation of HCHO was more important than direct emissions in Los Angeles, CA during the summertime days studied. However, in winter or at night and in the early morning, direct emissions can be more important (WEB_1, 2002). This was also observed in Japan, where the concentrations of formaldehyde in the central mountainous region were not associated directly with motor exhaust but rather were associated with the photochemical oxidation of anthropogenic pollutants occurring there through long-range transport (Satsumabayashi et al., 1995).

Ambient gas-phase formaldehyde concentrations have been extensively measured throughout the world (Table 2.1). Mean concentrations range from 0.05 to 9.11 μg m^{-3} and 0.05 to 27.5 μg m^{-3} in rural and urban areas, respectively.

Formaldehyde exhibited clear daily variations with maximum levels generally occurring in the afternoon and minimum at night (Cerqueira, 2003; Granby et al.1997; Possanzini et al., 2002).

Dry deposition is an important nighttime sink for formaldehyde (Christensen et al., 2000).

Photochemical production was found to affect the atmospheric levels for 80–90% in summer days. It dropped below 35% in the winter period, when direct emission from traffic largely predominated. The importance of formaldehyde as the major source of hydroxyl radicals in Rome was also assessed (Possanzini et al., 2002; Finlayson and Pitts, 1986).

It was suggested that motor vehicle exhaust is expected to be the most important direct source of carbonyl compounds particularly in urban atmosphere, which are also the key compounds of photo chemically generated air pollution (Ho et al. 2002).

Table 2.1 Concentration of HCOH in gas phase around the world (μg m^{-3})

Concentration (μg m^{-3})	Location	Area	Period	Reference
2.8±2.9	Langmiur, New Mexico, USA	Forested	Summer 1997	Fierro et al. (2004)
0.6-3.6	Balbina, Amazonia	Forested	March and April 1998	Kesselmeier et al. (2000)
0.05-9.11	Different sites, Canada	Rural	1989-1998	Chénier (2003)
4.1±1.7	New Mexico, USA	Rural	Summer 1997	Fierro et al. (2004)
1.7±1.0	Gopalpura, India	Rural	1995-1996	Khare et al. (1997)
1.9	Lille Valby, Denmark	Rural	May-July1995	Christensen et al. (2000)
22.15	Toronto, Ontario	Urban	July- August	Chénier (2003)
0.05-27.5	Different sites Canada	Urban	1989-1998	Chénier (2003)
21.6±7.2	Rome, Italy	Urban	June-July 1994-1996	Possanzini et al. (2002)
12.0±4.	Rome, Italy	Urban	January-March 1995-1997	Possanzini et al. (2002)
5.64±1.42	Hong Kong	Urban	Summer 1999	Ho et al. (2001)
2.82±1.35	Hong Kong	Urban	December 1999 and January 2000	Ho et al. (2001
1.5-11.4	Xalapa, Veracruz, Mexico	Urban	June, November, December 1997	Báez et al. (2001)
9.5±3.1	Parabiago, Milan, Italy	Urban	January 1999	Andreini et al. (2000)
8.9±1.9	Parabiago, Milan, Italy	Urban	Summer 1998, Summer 1999	Andreini et al. (2000)
0.8-4.4	Albany, NY, USA	Suburban	October 1991	Khwaja (1995)
5.9±1.3	Boffalora, Milan, Italy	Rural-Industrial	January 1999	Andreini et al. (2000)
7.5±2.7	Boffalora, Milan, Italy	Rural-Industrial	Summer1998, Summer 1999	Andreini et al. (2000)
1.1±0.6	Lille Valby, Copenhagen, Denmark	Semi-Rural	Winter	Granby et al. (1997)
3.1±0.8	Copenhagen, Denmark	Urban	Winter	Granby et al. (1997)

2.2.2. Particle phase concentrations

Most of the studies on HCHO in the atmosphere are about the measurement of gas phase concentrations. There are only a few studies on ambient particle phase concentrations (Klippel and Warneck, 1980; Deandrade et al. 1995; Liggio and McLaren, 2003). Previous studies indicated that the concentrations of particle phase HCHO are much lower than the gas-phase HCHO. Average particle-phase formaldehyde concentrations were measured as 40 and 65 ng m^{-3} for rural and urban air in Germany. In maritime air masses the concentration was lower than 2 ng m^{-3} (Klippel and Warneck, 1980). Particle-phase Formaldehyde concentrations were measured as 6.8-27.3 ng m^{-3} for Urban in Salvador, Bahia, Brazil, and 28.0-55.0 ng m^{-3} for bus station and tunnel as high polluted area in urban (Deandrade et al. 1993) (Table 2.2).

Table 2.2 Concentration of HCHO in atmospheric particles around the world (ng m^{-3})

Concentration	Location	Area	References
6.8-27.3	Salvador, Bahia, Brazil	Urban	Deandrade et al. (1993)
28.0	Salvador, Bahia, Brazil	Bus station and Tunnel	Deandrade et al. (1995)
63.0±27.0	Mainz, Germany	Urban	Klippel and Warneck (1980)
39.2±26.5	Deuselbach, Germany	Rural	Klippel and Warneck (1980)
2.9-41.6 18.0	Vancouver, Canada	Urban	Liggio and McLaren (2003)
6.8-73.4 33.9	Langley, Canada	Rural	Liggio and McLaren (2003)

2.3. Dry Deposition

The removal rate of atmospheric particles by dry deposition is a function of the physical (particle size, density) and chemical properties of the aerosol, meteorological conditions (temperature, wind speed, atmospheric stability) and surface characteristics (terrain, vegetation). The understanding of dry deposition of particles is far from complete due to the complex dependence of deposition on these parameters (Zhang et al., 2001; Seinfeld, 1986).

Current dry deposition estimation methods often use measured air concentrations and modeled dry deposition velocities. These models assume the dry deposition flux of particles (F_p) can be estimated by using an overall particle dry deposition velocity (V_p) and particle phase air concentration (C_p):

$$F_p=V_p.C_p \tag{2.5}$$

To date there has been no consensus on the appropriate dry deposition velocity to use in these types of models. Estimated (Kaupp and McLahlan, 1999; Hoff et al., 1996) and experimental (Yi et al., 2001; Odabasi et al., 1999; Cakan 1999; Franz et al., 1998; Tasdemir 1997; Holsen et al., 1991) dry deposition velocities of air pollutants range over an order of magnitude.

There are no previous studies reporting dry deposition fluxes of HCHO. Table 2.3 presents examples of deposition fluxes of some semivolatile organic compounds.

Table 2.3 Dry deposition fluxes of SOCs reported previously

Flux ($\mu g\ m^{-2}\ d^{-1}$)	Method	Compound	Location	Period	Reference
0.19±0.08	Dry deposition plates	PCBs	Chicago, IL, USA	June 1995-October 1995	Tasdemir et al. (2004)
120±28	Dry deposition plates	ΣPAHs	Chicago, IL, USA	June 1995-October 1995	Vardar et al. (2002)
144±60	Dry deposition plates	ΣPAHs	Chicago, IL, USA	June 1995-October 1995	Odabasi (1998)

2.4. Wet deposition

Air pollutants are absorbed by droplets in the atmosphere and are deposited by rain, snow, or fog. This is called wet deposition. The deposition of air pollutants with rainfall or snow is primarily determined by gravity. The larger aerosol particles (<1.00 nm) serve a cloud condensation nucleus, so that the aerosol provides a source of formaldehyde in cloud and rainwater (Klippel and Warneck, 1980). Rainwater HCHO concentrations have been commonly measured at different sites around the world. Some examples are presented in Table 2.4.

Concentrations of formaldehyde in rain ranged from 0.44 $\mu g\ l^{-1}$ (near Mexico City) to 3003 $\mu g\ l^{-1}$ during the vegetation burning season in Venezuela due to anthropogenic sources. Mean concentrations ranged from 77 $\mu g\ l^{-1}$ (in Germany) to 321 $\mu g\ l^{-1}$ (during the non-burning season in Venezuela). In snow, concentrations of formaldehyde ranged from 18 to 901 $\mu g\ l^{-1}$ in California (Environment Canada, 1999a).

A mean snow concentration of 4.9 $\mu g\ l^{-1}$ is reported for Germany. In fog water, concentrations of 480–17027 $\mu g\ l^{-1}$ have been measured in the Po valley, Italy, with a mean of 3904 $\mu g\ l^{-1}$ (Environment Canada, 1999a).

Table 2.4 Concentration of HCHO in rainwater around the world (μg l^{-1})

Concentration	Location	Area	Period	References
294	Chaguaramas, Venezuela	Rural	1990	Sanhueza et al. (1991)
45-1920 99	Los Angeles, USA	Urban	1985-1991	Sakugawa and Kaplan (1993)
132	Gopalpura, India	Rural, Tropical	Monsoon season July 1995 and August 1996	Khare et al. (1997)
12-333 95±63	Heraklion, Greece	Urban	September 1999-May 2000	Economou and Mihalopoulos (2002)
99±9	Wilmington, USA	Urban	June1996-February 1998	Kieber et al. (1999)
26-1350 207±216	Los Angeles, USA	Urban	1981-1984	Kawamura et al. (2001)
21±93	Galicia, Spain	Monitoring sites around a thermal power plant	August 1996-1997	Pena et al. (2002)
5-162	Florance, Italy	Semi-Urban	Spring1996	Largiuni, et al. 2002
30-443	Florance, Italy	Semi-Urban	Winter1996-1997	Largiuni, et al. 2002

Atmospheric deposition is a significant source of deposited HCHO since concentrations in rainwater are approximately three orders of magnitude higher than in surface waters (Kieber et al., 1990; Nuccio et al., 1995).

2.5. Air-Water exchange

The stagnant two-film model has been commonly used to estimate air-water gas exchange. According to the two-film model, mass transfer is limited by the rate of molecular diffusion through thin films of air and water on either side of the surface

(Schwarzenbach et. al 1993). The net flux (F_g, μg m^{-2} d^{-1}) is driven by the fugacity difference between air and surface water:

$$F_g = K_g (C_g - C_w H/RT) \quad (2.6)$$

where C_w and C_g are the water and air concentrations of HCHO (μg m^{-3}), H is the Henry's law constant (L atm mol^{-1}), R is the universal gas constant (0.08205 L atm mol^{-1} K^{-1}), and T is temperature at the air-water interface (K). The gas phase overall mass transfer coefficient (K_g, m d^{-1}) is related to individual mass transfer coefficients for the liquid and gas films, k_w and k_g, as follows:

$$1/K_g = (1/k_g) + (H/RTk_w) \quad (2.7)$$

Mass transfer coefficients of water vapor, oxygen (O_2) and carbon dioxide (CO_2) have been related to wind speed by many researchers (Schwarzenbach et al. 1993). O_2 and CO_2 are commonly used as reference substances to measure k_w since their gas exchange depends only on liquid phase resistance. Water vapor is usually used to measure k_g because its transfer is controlled by the gas phase.

Schwarzenbach et al., (1993) suggested that $k_{g(H2O)}$ is a direct function of wind speed and proposed the following equation based on previous observations of water evaporation rates:

$$k_{g(H2O)}(\text{cm } s^{-1}) = 0.3 + 0.2\, u_{10} \quad (2.8)$$

It was noted that because of the influence of D_a, $k_{g(H2O)}$ is also temperature dependent. However, this effect is neglected in this equation.

Recently, wind speed was empirically correlated to the mass transfer coefficients of several species for which transfer to the WSS is controlled by air-side resistance (Shahin

et al., 2002). The measured mass transfer coefficients (k_g) of nitric acid (HNO_3), water vapor (H_2O), sulfur dioxide (SO_2), and ammonia (NH_3) gases were divided by the square root of the respective diffusivity and regressed against wind speed 10 m above the water surface ($k_g/D_a^{0.5}$ vs. u_{10}) and the following relationship was obtained:

$$k_g = D_a^{0.5} (0.98\, u_{10} + 1.26) \qquad (2.9)$$

where, k_g is the mass transfer coefficient, cm s^{-1}, D_a is diffusion coefficient in air, cm^2 s^{-1}, and u_{10} is the wind speed 10 m above the WSS in m s^{-1} . The relationship given in equation (2.9) was developed based on wind speed range 0.8 to 6.0 m s^{-1}.

Mackay and Yeun, (1983) measured the volatilization rates of 11 organic compounds in a wind-wave tank. k_w values of organic compounds adjusted for O_2 and regressed against friction velocity (u^*) were determined during the experiments. Friction velocity in the resulting equation then was replaced with an equation ($u^* = (6.1+0.63u_{10})^{0.5}u_{10}$) which relates u_{10} to friction velocity in environmental conditions. The following equation was suggested for the calculation of $k_{w(O2)}$:

$$k_{w(O2)}(\text{cm s}^{-1}) = 1\text{x}10^{-4} + 1.75.10^{-4}(6.1 + 0.63u_{10})^{0.5}\, u_{10} \qquad (2.10)$$

The least squares fit for the data was performed assuming a zero intercept. The intercept in the above equation ($1\text{x}10^{-4}$ cm s^{-1}) was added based on the evaluation of previous studies suggesting a minimum k_w value for no-wind conditions.

Recently, experimental $k_{w(O2)}$ values for the WSS were plotted against wind speed and a second order curve was fit through the individual data points (Odabasi et al., 2001). The following relationship was obtained:

$$k_{w(O2)} = 1.62\text{x}10^{-3} + 2.23\text{x}10^{-4}\, u_{10} + 1.66\text{x}10^{-4}\, u_{10}^2 \qquad (2.11)$$

This $k_{w(O2)}$ model for the WSS was developed on wind speed range from 0 to 6.8 m s^{-1}.

According to the two-film model, mass transfer is limited by the rate of molecular diffusion through thin films of air and water on either side of the surface. Thus, mass transfer coefficients for water vapor and oxygen can be adjusted for other compounds using their diffusivities in air and water. Equations (2.12) and (2.13) (Schwarzenbach et. al., 1993) have been recommended to adjust individual mass transfer coefficients:

$$k_{g(compound)}\ (cm\ s^{-1}) = k_{g(H2O)}\ [D_{a(compound)}/D_{a(H2O)}]^{0.61} \qquad (2.12)$$

$$k_{w(compound)}\ (cm\ s^{-1}) = k_{w(O2)}\ [D_{w(compound)}/D_{w(O2)}]^{0.5} \qquad (2.13)$$

where D_a and D_w ($cm^2\ s^{-1}$) are the diffusivities in air and water, respectively.

Formaldehyde (HCHO) reacts substantially and reversibly with water to form methane diol ($CH_2(OH)_2$):

$$HCHO + H_2O \underset{k_d}{\overset{k_h}{\rightleftharpoons}} CH_2(OH)_2 \qquad (2.14)$$

where $K_h = k_h/k_d$, is the equilibrium constant, k_h is the hydration rate constant (s^{-1}), and k_d is the dehydration rate constant (s^{-1}). These reactions occur over time periods similar to those required for diffusive transfer across the water boundary layer resulting in a flux enhancement of formaldehyde. The flux enhancement of formaldehyde (Ψ) due to chemical reaction can be calculated as follows (Schwarzenbach et al., 1993; 2003):

$$\Psi = (K_h + 1)/[1 + (K_h/q).\tanh q] \qquad (2.15)$$

Where $q = (2t_w/t_r)^{1/2}$ is a non-dimensional parameter (reaction/diffusion parameter), $t_w = (D_w/k_w^2)$, $t_r = 1/(k_h+k_d)$ is the time of reaction (s), D_w ($cm^2\ s^{-1}$) is the diffusivity in water, k_w is the water-side individual mass transfer coefficient ($cm\ s^{-1}$).

The enhanced gas phase overall mass transfer coefficient ($K_{g(enhanced)}$, $cm\ s^{-1}$) can be calculated as:

$$1/K_{g(enhanced)}=(1/k_g)+(H/RTk_w\Psi) \quad (2.16)$$

Schwarzenbach et al. (2003) estimated that the flux enhancement of formaldehyde would range from 4 to 13 for wind speeds of 10 $m\ s^{-1}$ and 1 $m\ s^{-1}$, respectively.

The equilibrium constant (K_h), the hydration rate constant (k_h), and the dehydration rate constant (k_d) can be calculated as a function of temperature (T, K) (Winkelman et al., 2000; Winkelman et al., 2002):

$$K_h=\exp[(3769/T)-5.494] \quad (2.17)$$

$$k_h=2.05x10^5 \exp(-2936/T) \quad (2.18)$$

$$k_d=4.96x10^7 \exp(-6705/T) \quad (2.19)$$

Since formaldehyde is hydrated in water, a distinction needs to be made between the apparent Henry's law constant (H^*) and the intrinsic Henry's law constant (H) (Betterton and Hoffmann, 1988). The experimentally determined value is the apparent Henry's law constant, and this includes a term for the equilibrium constant (K_h). The three constants H^*, H and K_h are related by the following equations:

$$H = [HCHO]_g/[HCHO]_{aq} \quad (2.20)$$

$$H^* = \{[HCHO]_g/[HCHO]_{aq} + [CH_2(OH)_2]\} \quad (2.21)$$

$$K_h = [CH_2(OH)_2]/[HCHO]_{aq} \quad (2.22)$$

where $[HCHO]_{aq}$ is the concentration of free unhydrated formaldehyde dissolved in the aqueous phase and $[HCHO]_g$ is the is the concentration formaldehyde in gas phase. Total formaldehyde concentration in the aqueous phase is the sum of $[HCHO]_{aq}$ and the concentration of formaldehyde present in methane diol form $[CH_2(OH)_2]$. Rearrangement of equations (2.20)-(2.22) gives a direct relationship between H^*, H and K_h:

$$H = H^* (1+K_h) \quad (2.23)$$

The apparent Henry's law constant (H^*) values of formaldehyde previously were measured by Betterton and Hoffmann (1988). Based on the results of this study, apparent Henry's law constant can be calculated as a function of temperature (T, K):

$$\text{Ln } H^*(\text{L atm mol}^{-1}) = (-7032.7/T) + 15.549 \quad (2.24)$$

The diffusivity of organic compounds in air (D_a, $cm^2\ s^{-1}$) can be estimated using the method of Fuller. This method is the most accurate for nonpolar gases at low to moderate temperatures and diffusivity estimates match observations to within 10% (Lyman et al., 1993; Schwarzenbach et al., 1993). The method is based on the following correlation:

$$D_a = 10^{-3}\{T^{1.75}[(1/m_{air}) + (1/m)]^{1/2}/P[V_{air}^{1/3} + V^{1/3}]^2\} \quad (2.25)$$

where T is the absolute temperature (K), m_{air} is the average molecular mass of air (28.97 g mol^{-1}), m is the organic chemical molecular mass (g mol^{-1}), P is the gas phase pressure

(atm), V_{air} is the average molar volume of the gases in the air (~20.1 cm^3 mol^{-1}), and V is the molar volume of chemical of interest (cm^3 mol^{-1}) (V_{HCHO}= 26 cm^3 mol^{-1}).

Similar semi-empirical methods can be used to estimate the diffusivity in water (D_w, cm^2 s^{-1}). The Hayduk and Laudie method is recommended for the calculation of D_w, because it has been validated by a recently compiled database (Lyman et al., 1993). Generally, this approach yields results that are correct to within 10% (Schwarzenbach et al., 1993). The Hayduk and Laudie method is based on the following equation:

$$D_w = 13.26x10^{-5}/(\mu^{1.14}.V^{0.589}) \quad (2.26)$$

where μ is the solution viscosity in centipoise (10^{-2} g cm^{-1} s^{-1}) at the temperature of interest, and V is the molar volume of the chemical (cm^3 mol^{-1}).

CHAPTER THREE
MATERIALS AND METHODS

The details of sampling techniques and experimental methods used in this study are explained in this chapter.

3.1. Sampling program

Ninety-two concurrent ambient air and deposition samples were collected between May 2003 and April 2004 on a 4 m high sampling platform located on the Kaynaklar campus of the Dokuz Eylul University, Izmir, Turkey. Between May-July 2003, sampling time was 24 hours (n=14). Samples were collected during daytime (n=41) and nighttime (n=37) periods starting on July 24, 2003 until the end of the sampling program. Samples were also collected to determine the total suspended particles (TSP) and its organic matter content (OM). Samples were collected once in every six days when there was no precipitation.

The sampling site is located approximately 10 km southeast of Izmir's center (Figure 3.1). The campus is relatively far from any settlement zones or industrial facilities. There are residential areas located approximately 2 km southwest and a highway 0.5 km south of the sampling site. Land cover in the adjacent area is a young coniferous forest. There are steel plants, a petroleum refinery and a petrochemical industry located 45 km to the northwest. The nearest industrial facility is a cement work about 10 km at the north and an open road gravel storage site nearly 3 km at the east.

Deposition and ambient air samples were collected during successive daytime and nighttime (sunrise-sunset) periods. Twenty-seven rain samples were also collected manually during the rainy season in Izmir (October 2003-April 2004).

Meteorological data was obtained from a 10 m high tower located at the sampling site (Table 3.1). The tower was equipped with temperature, humidity, pressure, wind direction sensors, a rain gauge, and an anemometer (Davis Instruments, Australia) (Figure 3.2). The monitored parameters were stored in a data logger in 1 min intervals and downloaded to a computer located at the same site.

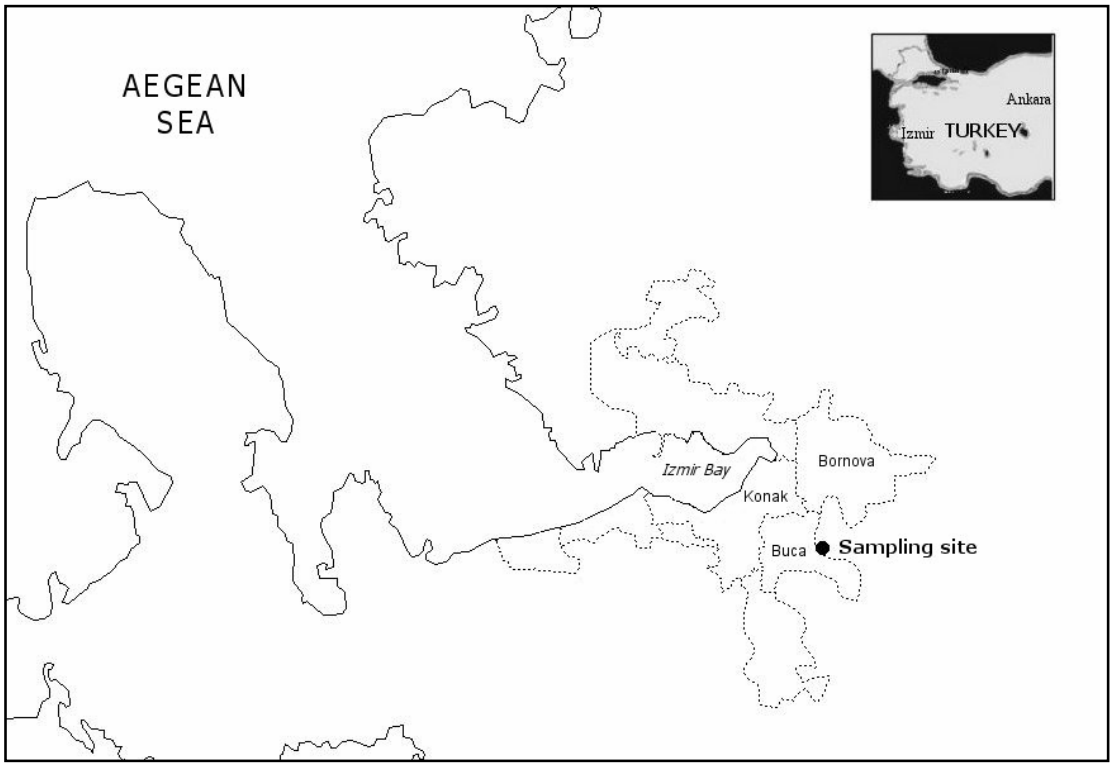

Figure 3.1 Location of the suburban sampling site

Figure 3.2 View of the sampling platform, sampling equipment and the meteorological tower

Table 3.1 Summary of meteorological, TSP and OM data

Sample Number	Date	Temperature (°C)	Relative Humidity (%)	Wind speed (m s^{-1})	C (TSP) (µg m^{-3})	C (OM) (µg m^{-3})	OM (%)
1	01-May-03	21	53	1.9			
2	07-May-03	20	46	5.3			
3	13-May-03	23	49	2.7			
4	28-May-03	19	70	2.2	193	106	55
5	03-Jun-03	22	45	2.3	54	25	47
6	16-Jun-03	27	52	2.6	92	43	47
7	22-Jun-03	25	35	5.6	75	34	46
8	28-Jun-03	27	32	4.6	68	24	35
9	04-Jul-03	29	41	2.8	63	35	56
10	07-Jul-03	28	32	9.4	64	17	27
11	08-Jul-03	27	36	7.4	89	70	79
12	09-Jul-03	26	38	6.5	56	24	42
13	10-Jul-03	27	33	6.2	75	25	33
14	16-Jul-03	29	31	7.5	63	28	45

Table 3.1 (Page 2 of 3)

Sample Number	Date	Temperature (°C)	Relative Humidity (%)	Wind speed (m s^{-1})	C (TSP) (µg m^{-3})	C (OM) (µg m^{-3})	OM (%)
15	18-Jul-03	31	31	5.5	70	37	53
16	24-Jul-03	30	30	6.1	65	39	60
17	24-Jul-03	25	52	2.5	47	38	81
18	30-Jul-03	30	35	6.1	42	24	58
19	31-Jul-03	24	63	1.4	71	45	64
20	02-Aug-03	30	45	4.4	77	35	46
21	03-Aug-03	25	62	0.7	74	39	53
22	03-Aug-03	29	52	5.3	69	38	55
23	04-Aug-03	25	61	3.4	50	25	50
24	12-Aug-03	29	32	7.1	134	59	44
25	13-Aug-03	23	34	7.3	51	20	40
26	21-Aug-03	30	25	7.7	73	28	39
27	25-Aug-03	24	49	0.9	63	24	39
28	25-Aug-03	29	36	3.1	102	34	33
29	26-Aug-03	24	45	1.5	50	24	48
30	01-Sep-03	31	35	3.6	99	36	36
31	02-Sep-03	25	62	2.1	93	8	9
32	06-Sep-03	21	34	6.3	65	38	59
33	07-Sep-03	18	44	4.8	23	13	55
34	07-Sep-03	22	31	7.4	47	38	81
35	08-Sep-03	18	47	6.6	49	45	92
36	16-Sep-03	21	47	6.2	50	23	45
37	17-Sep-03	18	60	5.7	41	22	53
38	23-Sep-03	24	42	2.8	80	48	60
39	24-Sep-03	19	76	0.6	76	47	61
40	02-Oct-03	22	40	7.2	45	9	20
41	03-Oct-03	18	63	3.2	80	27	33
42	08-Oct-03	18	69	2.2	53	27	50
43	08-Oct-03	23	51	6.1	79	64	80
44	14-Oct-03	20	40	7.0	140	64	46
45	15-Oct-03	16	53	3.5	87	33	38
46	21-Oct-03	24	58	6.8	54	21	39
47	22-Oct-03	20	69	3.4	23	16	67
48	01-Nov-03	21	60	4.5	28	3	10
49	02-Nov-03	16	90	2.1	67	22	33
50	02-Nov-03	23	57	2.1	37	22	58
51	03-Nov-03	19	63	2.0	64	28	43
52	07-Nov-03	14	77	6.2	41	29	71
53	08-Nov-03	13	77	6.7	38	26	68

Table 3.1 (Page 3 of 3)

Sample Number	Date	Temperature (°C)	Relative Humidity (%)	Wind speed (m s^{-1})	C (TSP) (µg m^{-3})	C (OM) (µg m^{-3})	OM (%)
54	12-Nov-03	9	57	3.3	87	64	73
55	13-Nov-03	7	62	4.1	51	46	89
56	13-Nov-03	10	53	2.9	36	25	69
57	14-Nov-03	6	69	2.8	144	129	89
58	18-Nov-03	16	72	2.3	44	16	36
59	19-Nov-03	13	81	2.3	84	42	50
60	19-Dec-03	5	48	5.0	102	85	83
61	28-Dec-03	4	85	1.3	28	17	59
62	28-Dec-03	9	70	0.6	117	80	69
63	29-Dec-03	6	82	1.5	72	65	90
64	29-Dec-03	11	68	2.2	30	18	60
65	12-Jan-04	5	88	3.7	58	45	77
66	13-Jan-04	8	82	8.1	63	60	95
67	04-Feb-04	7	59	9.2	17	11	67
68	05-Feb-04	4	67	7.4	26.	23	87
69	06-Feb-04	13	59	1.4	73	49	68
70	07-Feb-04	9	82	2.5	79	47	60
71	07-Feb-04	16	53	4.8	48	28	59
72	08-Feb-04	13	78	7.2	30	12	41
73	08-Feb-04	15	70	8.7	46	12	25
74	09-Feb-04	12	84	6.4	21	16	75
75	02-Mar-04	11	77	2.2	30	19	63
76	02-Mar-04	14	61	3.0	46	13	28
77	14-Mar-04	11	41	7.0	36	10	27
78	15-Mar-04	6	67	6.3	61	20	32
79	17-Mar-04	13	34	8.2			
80	18-Mar-04	10	56	1.9			
81	18-Mar-04	13	56	7.0			
82	19-Mar-04	10	61	5.6			
83	19-Mar-04	13	45	6.0			
84	20-Mar-04	11	60	1.4			
85	05-Apr-04	14	32	2.3			
86	06-Apr-04	9	55	1.7			
87	07-Apr-04	15	67	7.5			
88	08-Apr-04	13	78	5.3			
89	28-Apr-04	15	68	4.1	60	18	31
90	28-Apr-04	12	86	1.7	61	47	78
91	29-Apr-04	16	65	4.7	91	40	44
92	29-Apr-04	13	68	2.1	63	45	71
Average		18	56	4.4	64	35	54
SD		8	17	2.3	30	22	20

3.2 Sampling Method

The following instrument combination was used during the sampling program:

a) A water surface sampler, (particle and gas phase dry deposition flux).
b) Five dry deposition plates (particle phase dry deposition flux).
c) Ambient air sampling train (ambient gas phase concentration).
d) A high-volume sampler (ambient particle phase concentration)
e) A high-volume sampler (total suspended particulate matter and its organic matter content).
f) A wet deposition collector.

3.2.1 Water surface sampler

Total (particulate+gas) formaldehyde fluxes were measured using an aerodynamically smooth circular water collection surface, which has a water replenishing system to maintain a constant water level. Water enters the water surface from its center and overflows from the triangular weirs located at the sides (Figure 3.3).

The water surface holder has an airfoil shape with a leading edge to minimize airflow disruptions caused by collector geometry. The water surface plate (37.2 cm diameter 0.65 cm depth) was made of stainless steel. It is placed inside the holder at a height which allows the water on the plate to be at the same level with the top of the water surface holder.

Before the field sampling program, two water surface samplers were used concurrently in laboratory experiments. One of them was run with water circulation, the other without water circulation. Initially, 500 ml DI water was added to the water surface plate of the WSS without circulation and water was added occasionally if significant evaporation was observed. The HCHO fluxes measured with these two

samplers were not statistically different (at the 95% confidence level). Running the WSS with circulation requires using at least 2.5 L water for sampling. During the preliminary field experiments using 2.5 L water resulted in dilute concentrations and detection problems. Therefore, the WSS run without water circulation during the sampling program.

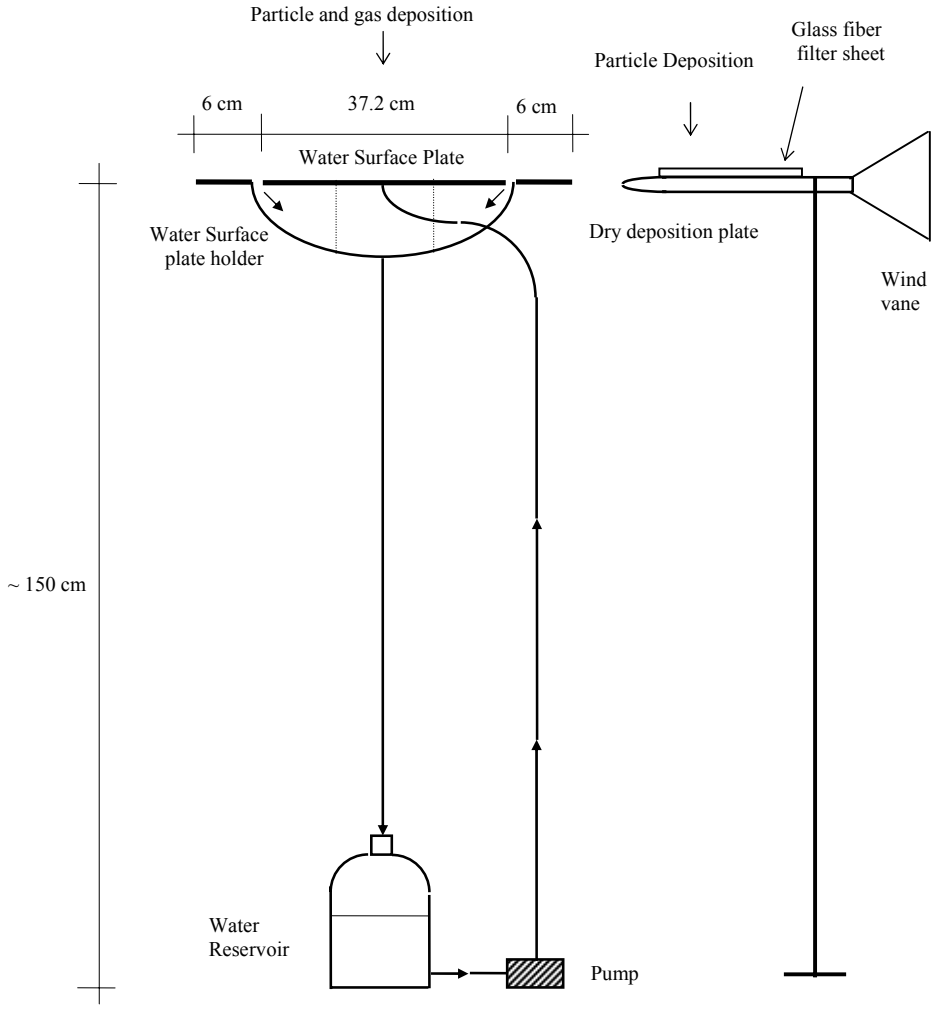

Figure 3.3 Water surface sampler (WSS) and dry deposition plate that were used to measure total (particle+gas) and particle formaldehyde dry deposition.

3.2.2 Dry deposition plate

The particle dry deposition flux was measured using a smooth deposition plate (22x7.5 cm) with a sharp leading edge, mounted on a wind vane (Figure 3.3). Glass fiber filter (GFF) sheets mounted with cellulose acetate strips on the plates were used to collect the deposited particles. The dimensions of the GFF sheet's deposition surface were 5.5x12 cm. Five plates and sheets with a total collection area of 330 cm^2 were used for sampling.

3.2.3 Ambient air sampling train

Gas phase atmospheric formaldehyde was collected using a sampling train consisting of a filter holder, two impingers in series, a vacuum pump and a rotameter and gas meter (Figure 3.4).

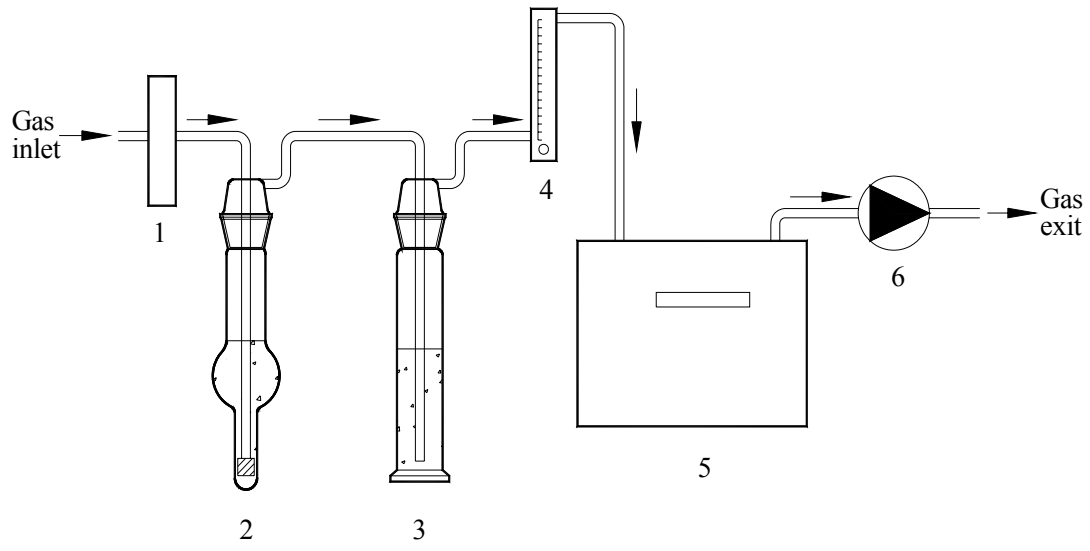

Figure 3.4 Schematic layout of ambient air sampling train. (1) Filter holder, (2) First impinger as absorber, (3) Second impinger as backup absorber, (4) Rotameter, (5) Gasmeter, (6) Vacuum pump.

Air was first drawn through a 47 mm glass fiber filter to remove particles and then, through two impingers connected in series. Gaseous HCHO is absorbed in the first and second impingers filled with 75 and 50 ml deionized water, respectively. Then, air flowed through a rotameter and a dry gas meter used for flow rate and sampling volume monitoring. Average sampling time was 12 h. The average sampling volume was 1.15±0.40 m^3 for gaseous formaldehyde samples.

3.2.4 Particulate formaldehyde

Particulate formaldehyde was collected on glass fiber filters using a high volume sampler, Model GPS-11 (Thermo-Andersen Inc.). Particles were collected on 10.5-cm diameter quartz filters. For some sampling periods a backup filter was also used to evaluate the sampling artifacts (i.e., gaseous formaldehyde adsorption, particle penetration). Average sampling time was 12 h. The average sampling volume was 179±54 m^3 for particulate formaldehyde samples.

3.2.5 Total suspended particulate matter (TSP)

Concurrently, particulate samples were collected on 11-cm diameter glass fiber filters using another high volume sampler to determine total suspended particulate matter (TSP) and its organic matter (OM) content. Average sampling time was 12 h. The average sampling volume was 49±16 m^3 for TSP samples.

3.2.6 Wet deposition collector

Rainwater samples were collected for 27 rain events between September 2003 and April 2004 on the sampling site using a metallic collector with a surface area of 0.109 m^2 drained into an amber glass bottle. Rainwater collector and glass bottle were rinsed several times with DI water before sampling. Rainwater sampling controlled

manually. After sampling, rainwater volume measured and collected. The sample was filtered and analyzed immediately after collection.

3.3 Laboratory Experiments

3.3.1 Laboratory experiments to determine the overall mass transfer coefficient of formaldehyde

In addition to field studies, HCHO air-water exchange flux and concurrent gas-phase concentration measurements were conducted in the laboratory. Gaseous formaldehyde fluxes were measured using the WSS. The first set of experiment was conducted at elevated HCHO concentrations. In order to increase the formaldehyde concentration artificially, 37% formaldehyde solution was placed into a beaker and it was left open. Evaporated HCHO from the beaker provided the required elevated indoor concentrations. High concentrations were used to shorten the sampling periods and minimize the probable loss of deposited HCHO. In this set of experiments sampling time was 60 min, temperature was 16-8 °C and humidity was 60-77%.

In the first set of indoor experiments, wind was provided using an adjustable fan located at a 2 m horizontal distance from the WSS. The variation of wind speed over the WSS was measured using a vane anemometer (Testo 451) at several points through a 40x20 cm vertical section. Fifteen samples were collected under different wind conditions: calm (n=3), 1 m s^{-1} (n=4), 1.6-1.7 m s^{-1} (n=4), 2-2.4 m s^{-1} (n=4). The relative standard deviation of wind speed through the section was less than 5%, indicating a uniform wind was provided for the experiment.

The second set of indoor experiment was conducted using a wider wind speed range and lower HCHO concentrations. As in the previous series, the formaldehyde concentration in the indoor air was artificially increased. However, this time to get lower concentrations, the 37% Formaldehyde solution was placed in a 25 ml flask having a

much lower opening than the beaker used in the first set of experiment. Sampling time was 120 min, temperature and humidity were 18 °C and 75-80% respectively. Wind speeds were calm, 1, 2, 3, and 3.5 m s^{-1}. The experiments were run in triplicate at each wind speed (n=15).

3.3.2 Laboratory experiments to determine sulfite interference with HCHO analysis

Sulfite (SO_3^{2-}) and bisulfite (HSO_3^-) react with formaldehyde to form hydroxymethane sulphonate (HMS^-, $CH_2(OH)SO_3^-$) (Winkelman et al., 2000; Kieber et al., 1999). When formaldehyde is removed during the DDL (diacetyl dihydrolutudin) development in analysis, the HMS^- decomposes. For small concentrations of sulfite the decomposition is fast enough and the analysis remains unaffected. A noticeable reduction of DDL after a reaction time of 30 min was reported for sulfite concentrations greater than 10^{-5} M (Klippel and Warneck, 1980). The HMS^- can be destroyed by oxidation of sulfite with iodine, and the interference with DDL formation is removed (Klippel and Warneck, 1980; Economou and Mihalopoulos, 2002).

The interference of sulfite with HCHO analysis was investigated by spiking HCHO containing solutions (0.1, 0.3, 0.5, and 1.0 μg ml^{-1}) with $3.3x10^{-5}$, $9.9x10^{-5}$, $1.7x10^{-4}$, $3.3x10^{-4}$, $1.7x10^{-3}$ M Na_2SO_3 (n=20). Having the same concentrations, another series of solutions was prepared and iodine was added into these samples (n=20). Both series of solutions were analyzed for formaldehyde by Nash method as described in Section 3.7.

3.3.3 Determination Henry's Law Constant of Formaldehyde

In this study, the Henry's law constant of formaldehyde was measured at six different temperatures, using gas-stripping technique that was previously applied by Betterton and Hoffmann (1988).

The gas-stripping apparatus consisted of a 75 cm by 5 cm diameter water-jacketed glass reactor filled with 1 L deionized water (Figure 3.5). The water depth was 50 cm and the temperature of striping column adjusted using a temperature controlled circulating water bath. Before pumping, this pure N_2 gas was passed through gas washing bottle filled with deionized water in order to saturate the N_2 with water vapor. Once the formaldehyde was added to the reactor and mixed, 200 ml min^{-1} compressed N_2 gas was pumped through a medium porosity (40 μm) sintered glass frit from the bottom of the reactor. Vapor phase HCHO passed through an impinger where it was trapped by 50 ml deionized water. A backup impinger was placed into the sampling train to check if there was a breakthrough. In all cases HCHO was below the detection limit. Then, the gas was drawn through a silica gel column for drying and through a high-resolution flowmeter.

Water samples (1 ml) were drawn through a valve located at the base of the reactor at the start and end of each experiment. Above mentioned procedure was applied at six different temperatures (50, 40, 30, 20, 10 and 5°C) and replicated three times for each temperature. For the experiment at 50 °C runtime was 60 minutes for other temperatures it was 120 min. Samples were analyzed immediately using the Nash method.

H^{*}, was calculated as follows:

$$H^{*}, = C_g/[(C_{w(n)} + C_{w(n+1)})/2] \quad (3.1)$$

where C_g (μg ml^{-1}) is the time-integrated gas-phase HCHO concentration and $C_{w(n)}$ and $C_{w(n+1)}$ (μg ml^{-1}) are the dissolved formaldehyde concentrations measured at the beginning and end of air sampling period, respectively.

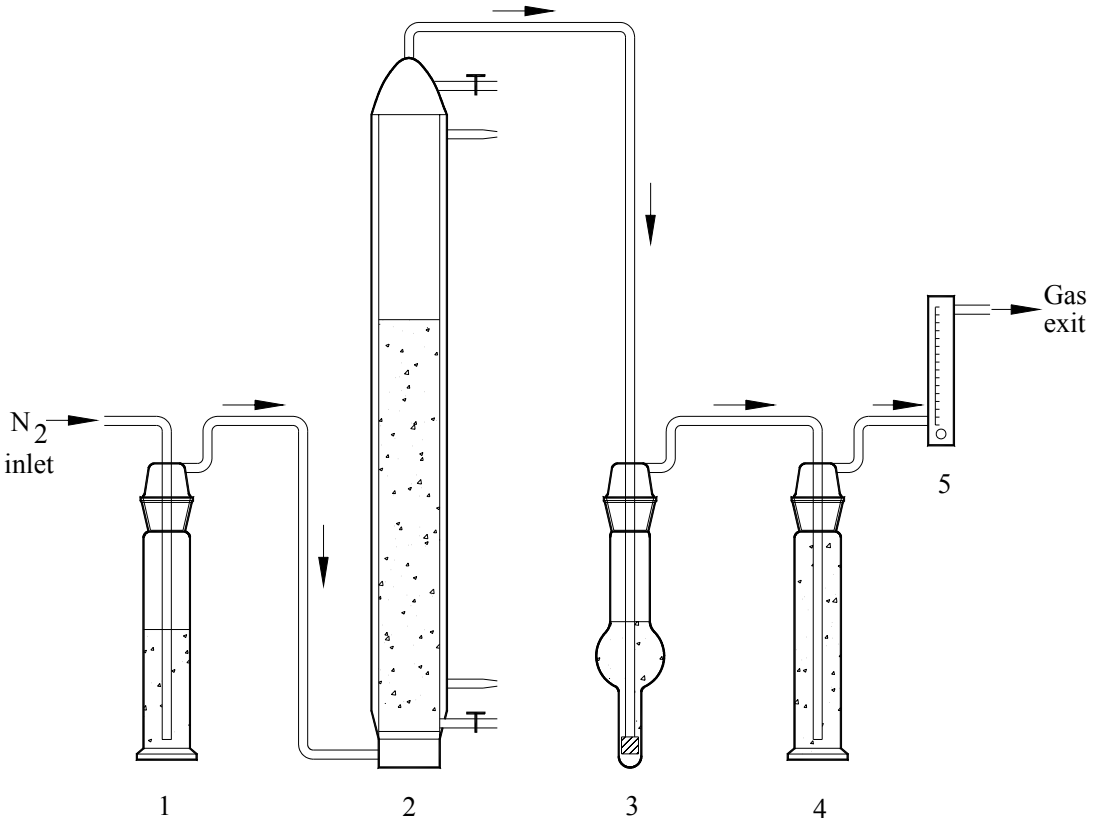

Figure 3.5. Schematic layout of Henry's law constant's experimental train. (1) Conditioner, (2) water jacketed stripping column, (3) impinger as absorber, (4) impinger filled with silica gel for gas drying, (5) Rotameter.

3.4 Preparation for Sampling

3.4.1 Glassware

Glassware washed with concentrated H_2SO_4, several times with tap water and deionized water and dried in oven at 105 °C for overnight. The openings of the glassware were covered with aluminum foil as soon as they were removed from the oven.

3.4.2 HDPE Containers

High Density Polyethylene (HDPE) containers were used for collection of the water samples. HDPE containers were washed with concentrated H_2SO_4, and several times with tap water and finally with deionized water.

3.4.3 Glass Fiber Filters

Glass fiber filters were wrapped loosely with aluminum foil and baked in a furnace at 450 °C overnight. Then they were allowed to cool to room temperature in a desiccator.

3.4.4 Dry Deposition Plates

Plates and cellulose strips were cleaned with detergent and hot water, rinsed with tap water several times and then with DI water. Then, they were wiped with dust free paper and wrapped with aluminum foil until use. Glass fiber filter sheets (7.5x12 cm) were mounted on dry deposition plates and both sides covered with cellulose acetate strips (1x12 cm).

3.4.5 Water Surface Sampler

All wetted components of water surface sampler were rinsed with DI water after and before sampling.

3.4.6 Sample Handling

All prepared materials for sampling such as dry deposition plates, glass fiber filters, HDPE sample containers were transported to the field in closed containers to avoid

exposure. Likewise samples were transported to the laboratory in closed containers to protect loss of material.

3.5 Preparation for Analysis

Particulate formaldehyde was extracted from filters with DI water. The filter and dry deposition plates were added with DI water in flasks and extracted in an ultrasonic bath for half an hour. Then, the extract was filtered through a 0.45 μm membrane filter. WSS samples were filtered through a 0.45 μm membrane filter before they were analyzed.

3.6 Formaldehyde analysis

Formaldehyde was analyzed using the Nash method (Nash, 1953). This technique has been successfully used in the past (Sanhueza et al., 1991; Khare, et. al., 1997, Economou and Mihalopoulos, 2002). Analyses were performed with a 1:8 mixture of the Nash reagent (0.02 M acetylacetone, 0.05 M acetic acid, 2 M ammonium acetate buffer) and sample. The yellow colored product diacetyl dihydrolutidin (DDL) formed by the reaction of Nash reagent with formaldehyde is determined by spectrophotometry at the maximum of its absorption at 412 nm. Reagent and sample mixtures were hand mixed and placed into a water bath maintained at 50 °C. The reaction is completed after 2 h. The interference of higher aldehydes is negligible, since they react with the Nash reagent more slowly and also their absorption spectra are shifted with respect to 412 nm (Klippel and Warneck, 1980).

Preparation and standardization of formaldehyde stock solution

Standardization of formaldehyde was done according to NIOSH Manual of Analytical Techniques, Method 3500.A HCHO solution (2.7 ml, 37%) is diluted to 1 l with deionized water. This solution is stable for at least three months. Five ml of freshly prepared 1.13 M sodium sulfite solution is placed into a 50 ml beaker and stirred

magnetically. Solution pH is adjusted between 8.5 and 10 with base or acid and recorded. Ten ml of formaldehyde solution is added. Then, pH should be about 11. The solution is titrated back to its original pH with 0.02 N sulfuric acid (1 ml acid = 0.600 mg HCHO; about 17 ml acid needed). If the endpoint pH is overrun, the solution is back-titrated to the endpoint with 0.01 N sodium hydroxide and spent volume of acid solution is corrected.

The concentration, C_s (mg ml^{-1}), of the formaldehyde stock solution is calculated as:

$$C_s = (30.0\ (N_a.V_a - N_b.V_b))/V_s \qquad (3.2)$$

where:
30.0 = 30.0 g/equivalent of formaldehyde
N_a= normality of sulfuric acid (0.02 N)
V_a= volume of sulfuric acid (ml) used for titration
N_b= normality of NaOH (0.01 N)
V_b= volume of NaOH (ml) for back-titration
V_s= volume of formaldehyde stock solution (10.0 ml).

Standard curves prepared daily at 0.0, 0.1, 0.3, 0.5, 1.0, 2.0, 3.0 μg ml^{-1} HCHO concentrations. All liquid phase samples (water from the WSS, ambient gas-phase absorbing solution, and filter and plate extracts) were analyzed for formaldehyde using the Nash method. Sixteen ml samples and 2.0 ml of a solution (mixture ratio is 8/1), containing 0.02 M acetylacetone, 0.05 M acetic acid, and 2.0 M ammonium acetate were added to a flask. Reaction mixtures were hand mixed and placed in a 50°C bath for 2 h. Absorbance was measured at 412 nm.

3.7 Determination of TSP and organic matter content

Prior to sampling for TSP, glass fiber filters were wrapped loosely with aluminum foil and they were baked overnight at 450 ºC in a muffle furnace to remove any organic residues. They were then allowed to cool to room temperature in a desiccator and were weighed using a micro balance capable of weighing 0.1 mg. After sample collection filters were kept in a desiccator overnight and they were reweighed. TSP was determined by subtracting the initial weight from the final weight. To determine the organic matter content of the particles, filters were then baked for 1 h at 450 ºC in a furnace, allowed to cool to room temperature in a desiccator, and weighed. Organic matter was determined by subtracting the final weight (after baking) from the initial weight (before baking) of the used filters.

3.8 Quality Assurance/Quality Control

3.8.1 Sample Collection Efficiency

Deionized water has been used for HCHO sampling. Sampling flow and average volume was 1500 ml min^{-1} and 1.15±0.40 m^3 respectively. Seventy five and 50 ml DI water was added into the first and second impingers. The average HCHO amount was 21.6±8.8% in the second impinger. In the third impinger that was tested several times, HCHO was below the detection limit. These results indicated that breakthrough was not a problem during sample collection.

3.8.2 Calibration Standards

Calibration curves prepared daily using seven concentration levels (0.0, 0.1, 0.3, 0.5, 1.0, 2.0, 3.0 μg ml^{-1}) of HCHO concentrations. The r^2 of the calibration curves was higher than 0.999. An example of the calibration curve is presented in Figure 3.6.

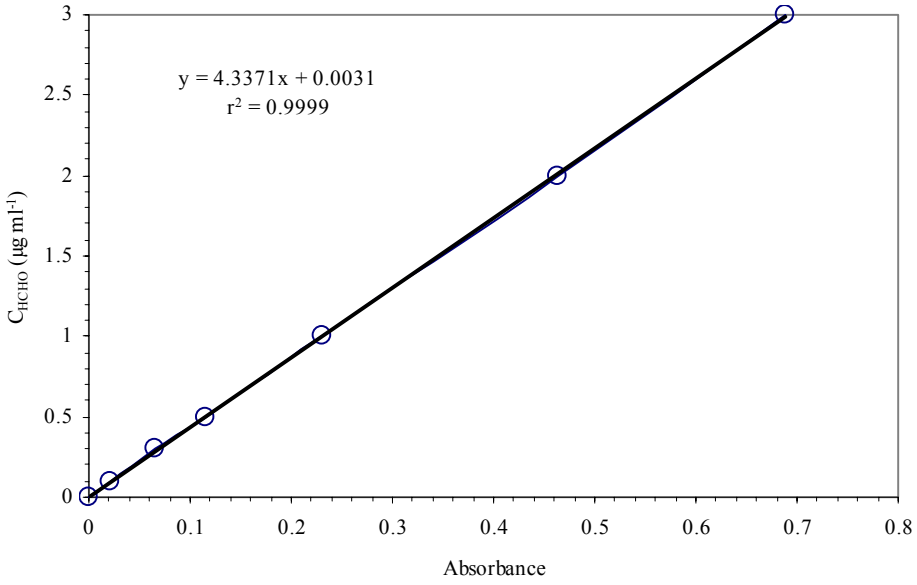

Figure 3.6 Example calibration curve for formaldehyde analysis

3.8.3 Water Surface Samplers

Before the field sampling program, two water surface samplers were used concurrently in laboratory experiments. One of them was run with water circulation, the other without water circulation. Initially, 500 ml DI water was added to the water surface plate of the WSS without circulation and water was added occasionally if significant evaporation was observed. The HCHO fluxes measured with these two samplers were not statistically different (at the 95% confidence level). Running the WSS with circulation requires using at least 2.5 L water for sampling. During the preliminary field experiments using 2.5 L water resulted in dilute concentrations and detection problems. Therefore, the WSS was run without water circulation during the sampling program. Recent studies indicated that particulate dry deposition flux of some organic and inorganic species (PAHs, lead, and calcium) was statistically the same as found with

deposition plate and WSS techniques, indicating that both of these surrogate surfaces have similar characteristics for atmospheric particle collection (Odabasi et al., 1999; Yi et al., 1997). The measured fluxes with co-located samplers were also statistically the same (at the 95% confidence level) and the differences in duplicate samples were less than 10% (Odabasi et al., 1999; Hsu, 1997).

3.8.4 Blanks

Field blanks were analyzed to determine the amount of contamination from sample collection and preparation. Field blank concentrations were below the detection limit of the method.

3.8.5 Detection limit

Economou and Mihalopoulos (2002) reported the detection limit of the Nash method as 0.0051 μg ml^{-1} and the reproducibility defined as the relative standard deviation of six consecutive measurements of the same sample better than 3%. It was also reported that the applied method is linear in the range 0.4 (detection limit)–2000 μg l^{-1} and linear regression of standards is $r^2 > 0.9998$ with a reproducibility better than 3% (Largiuni et al. 2002). In the present study, detection limit of the method was determined as 0.0075 μg ml^{-1} similar to one reported by Economou and Mihalopoulos (2002).

3.8.6 Organic matter content

It is possible that the determination of OM content by the method used in this study may be interfered by the weight loss of glass fiber filters at high temperatures. The hourly weight loss of filters at 450 ºC with time was monitored for 12 hours. It was observed that the maximum weight loss (3 mg) occurs within a 2 h period and the weight loss decreases to 0.3 mg h^{-1} and becomes stable for the remaining period. To minimize the interference from weight loss of filters at high temperatures in OM

determination, concurrent blank filters were run for each sample. Determined OM contents were corrected using the weight loss in blank filters during baking. The average weight loss of blank filters (0.3 mg) was significantly lower than the average weight loss of the samples (2.2 mg) indicating that the interference was not significant in OM determination.

3.9 Calculations

Ambient air concentrations were calculated as follows:

$$C(\mu g\ m^{-3}) = m/V \quad (3.3)$$

where m (μg) is the analyte mass in the sample, and V (m^3) is the sampled air volume.

Dry deposition fluxes (F, μg m^{-2} d) were calculated from analyte mass (m, μg), collection area of sampler (A, m^2) and sampling time (t, d):

$$F = m/A.t \quad (3.4)$$

F_t=Total(particulate+gas) dry deposition flux (water surface sampler)

F_p=Particulate phase dry deposition flux (dry deposition plate)

The gas phase dry deposition fluxes were calculated by subtracting the particulate phase fluxes measured with dry deposition plate (F_p) from total (particulate+gas) fluxes (F_t) measured with the WSS:

$$F_g = F_t - F_p \quad (3.5)$$

Particulate phase dry deposition velocities (V_p, cm s^{-1}) were calculated using the dry deposition fluxes measured with dry deposition plate and the particulate phase air concentrations.

$$V_p=F_p/C_p \quad (3.6)$$

Gas phase overall mass transfer coefficients were calculated using the gas phase fluxes and concentrations:

$$K_g=F_g/(C_g - C_wH/RT) \quad (3.7)$$

It was assumed that the formaldehyde concentration in water (C_w) was zero. Validity of this assumption will be discussed in Chapter 4.

CHAPTER FOUR
RESULTS AND DISCUSSION

4. Results and Discussion

This chapter presents the ambient concentrations of HCHO, the distribution between gas and particle phases, dry and wet deposition fluxes, and air-water exchange. Experimental particle phase dry deposition velocities and overall gas phase transfer coefficients were calculated using the measured fluxes and concentrations. Experimental overall gas phase transfer coefficients were compared to those estimated using the two-film model with and without chemical enhancement.

4.1. Ambient Concentrations

4.1.1. Gas phase concentrations

Average gas phase formaldehyde (HCHO) concentrations (C_g) ranged from 1.1 to 36.9 μg m^{-3} (7.3±6.5 μg m^{-3}, average± SD) (Figure 4.1). These concentrations were within the ranges previously measured at different sites around the world (Table 2.1). By comparison, the rural site formaldehyde concentration measured by others were 4.1±1.7 μg m^{-3} (Fierro et al., 2004) in New Mexico, USA, 1.7±1.0 μg m^{-3} (Khare et al., 1997) in Gopalpura, India, a range of 0.05-9.1 μg m^{-3} was measured at different sites in Canada (Chénier, 2003). Ambient concentrations were also reported as daytime and nighttime and they were 8.0±6.1, 4.3±3.6 μg m^{-3} (average±SD), respectively. Daytime concentrations were generally higher and diurnal variation ratio of HCHO was 1.9±1.3.

A six-day sampling program was also conducted at an urban site to compare the urban and suburban concentrations. The urban sampling site was located 30 m away from a busy highway. Concurrent 24 h samples were collected in March 2004 in urban and in suburban (campus) sites. Average HCHO concentrations were 11.3±4.2 and 2.8±0.4 μg m^{-3} in urban and campus sites, respectively (Figure 4.2).

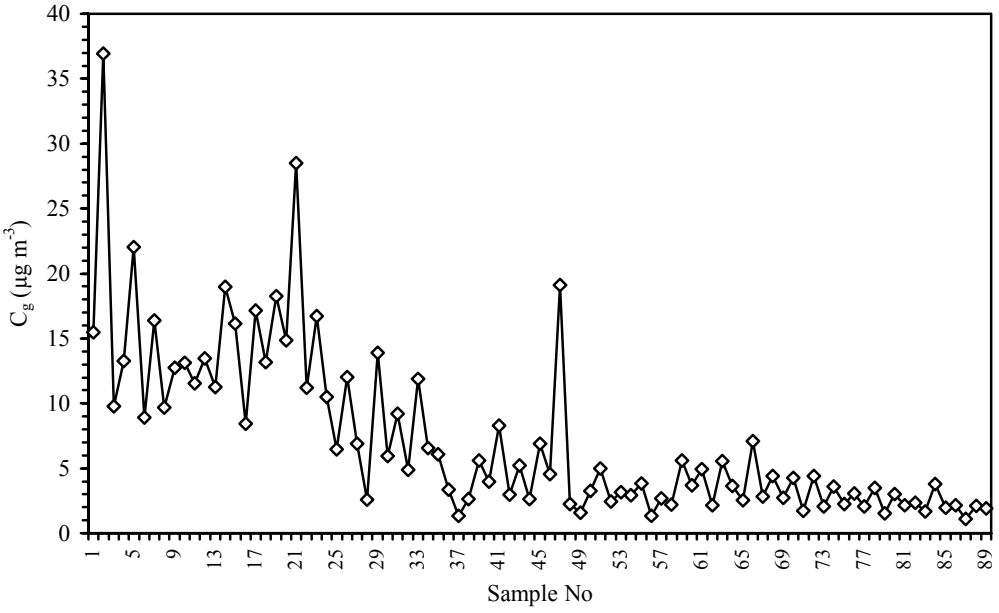

Figure 4.1 Variation of ambient HCHO concentrations during the sampling period.

On the average, urban concentrations were 4.1 times higher than the suburban concentrations. Since during the urban sampling program photochemical activity was low because of season, observed higher urban concentrations were probably due to the proximity of emission sources (traffic and residential heating).

Figure 4.3 shows the relationship between HCHO concentrations and ambient temperatures during the sampling program. HCHO concentrations were significantly correlated to the temperature (r^2=0.45, p<0.01). The periods with higher temperatures correspond to days when the incoming solar radiation and photochemical activity is

high. Therefore, the significant correlation between HCHO and temperature suggested that measured concentrations were affected by atmospheric photochemical reactions.

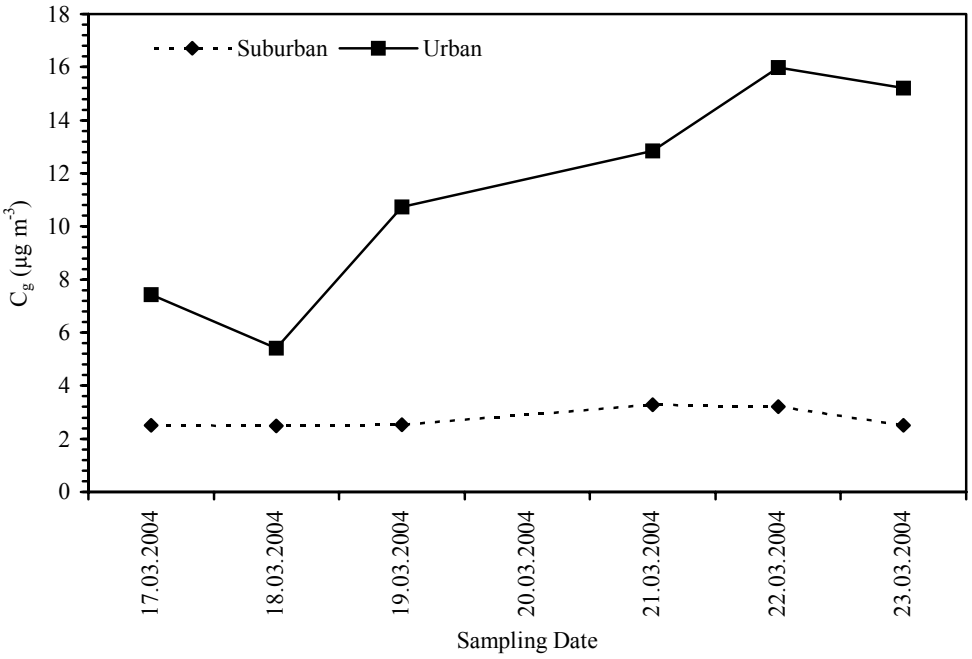

Figure 4.2 Urban and suburban HCHO concentrations during the March 2004 sampling program

However, emissions of HCHO have also diurnal and seasonal variations. Emissions from motor vehicles decrease during nighttime. Emissions from residential heating increase during the winter. As a result, the relationship between the temperature (or photochemical activity) and ambient HCHO concentrations is complicated. Therefore, the relationship between daytime and nighttime HCHO concentrations and temperature was also investigated excluding the 24 h samples (n=14) (Figure 4.4). Daytime and nighttime HCHO concentrations were also significantly and positively correlated to the temperature (p<0.01) suggesting that atmospheric HCHO was mainly affected by the photochemical reactions during relatively warmer periods.

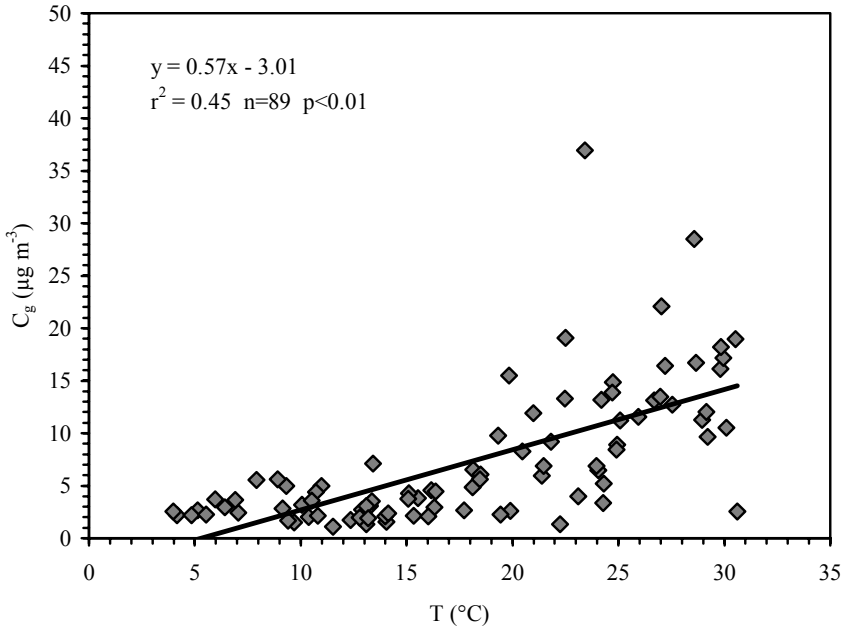

Figure 4.3 Relationship between ambient gas-phase HCHO concentration and temperature

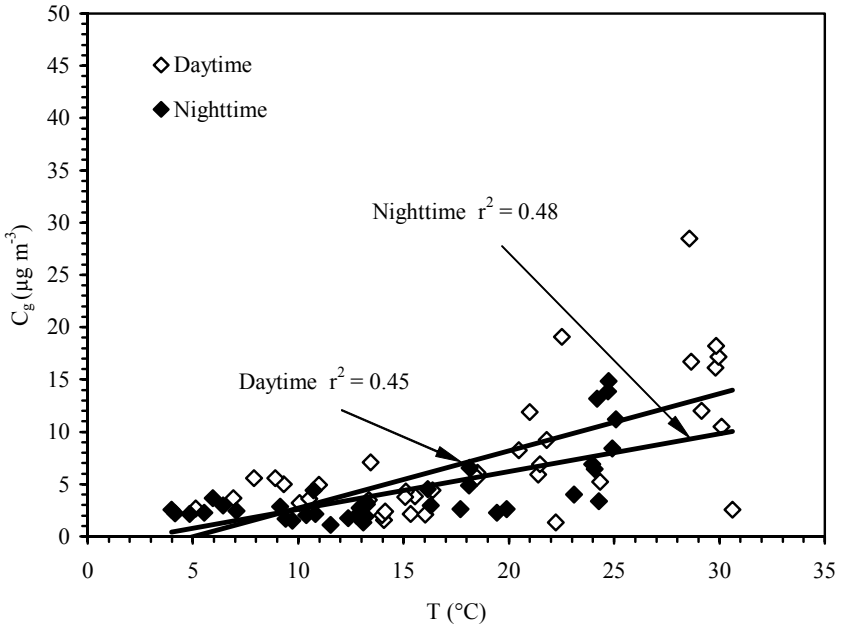

Figure 4.4 Variation of daytime and nighttime HCHO concentrations with temperature

4.1.2 Particle phase concentrations

Particle phase HCHO concentrations ranged between 3-65 ng m^{-3} (average±SD, 18±12 ng m^{-3}) (Figure 4.5). These concentrations were within the ranges previously measured at different sites around the world (Table 2.2). By comparison, average particle-phase formaldehyde concentrations were measured as 40 and 65 ng m^{-3} for rural and urban air in Germany (Klippel and Warneck, 1980). Liggio and McLaren (2003) recently reported a range of 3-42 ng m^{-3} for an urban area (Vencouver, Canada).

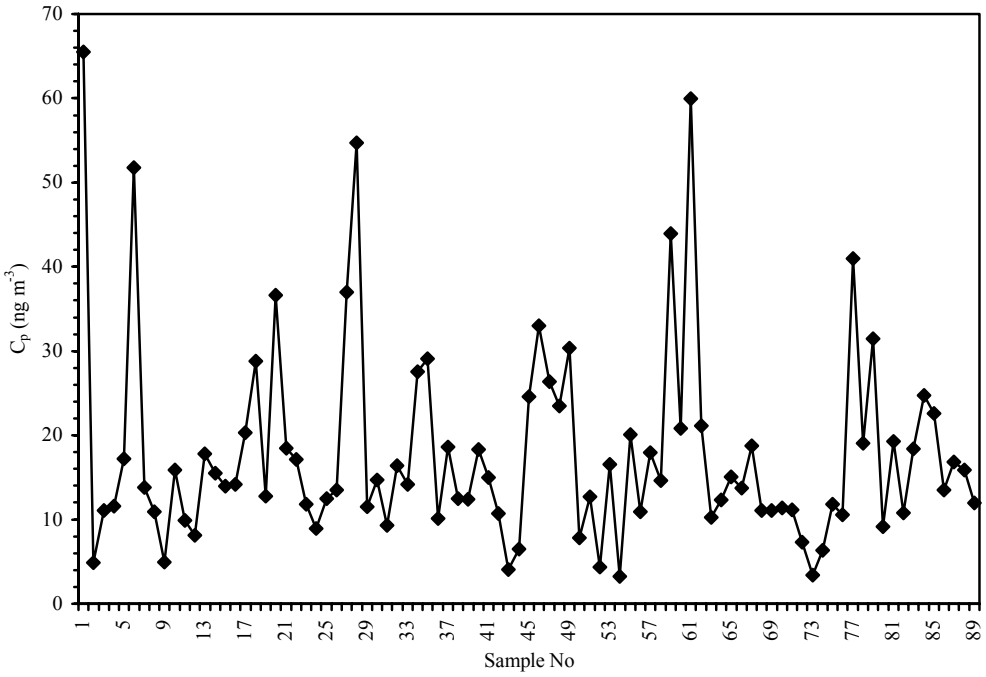

Figure 4.5 Variation of particle phase formaldehyde during the sampling program

Sampling artifacts associated with the glass fiber filters may influence the apparent gas-particle distribution of HCHO. Gas-phase HCHO may adsorb to the filter and particles collected on the filter or HCHO may be desorbed from the collected particles

by continuing gas flow if the gas-phase concentration decreases or if the temperature increases during the sampling period. The extent of sampling artifacts is often estimated using a backup filter. The sampling artifacts associated with particulate HCHO were previously evaluated by Klippel and Warneck (1980) based on some theoretical calculations, correlations between relative humidity and the HCHO amount on the backup filters, and correlations between sampling volume and amounts on the backup filters. They concluded that the amount of HCHO found on the backup filter was due to gas phase adsorption onto the filter, not due to particle penetration.

Backup filters were also used during 27 sampling periods in this study. The average amount found on the backup filters was 36% of the amount found on the first filters. However, the HCHO amounts found on the backup filter were not correlated with gas phase concentration and weakly correlated with relative humidity (r^2=0.13). The correlation between the HCHO amounts found on the backup filter and sampling volume was also weak (r^2=0.24). However, the HCHO amounts found on first and backup filters were correlated with each other (r^2=0.51) suggesting that the amounts detected on the backup filters may have been affected by particle penetration. Based on the results obtained in this study, it is not clear whether the adsorption of gas phase onto the filter or particle penetration is responsible for the HCHO observed on the backup filters. Therefore, the HCHO amounts found on the filters were not corrected for sampling artifacts. Since the sampling was conducted during relatively short periods (12 h, day or nighttime), the temperature fluctuations and sampling artifacts due to temperature changes were minimized in the present study.

4.1.3 Gas/Particle Phase Distribution

Particle/gas phase distribution of HCHO is an important factor in determining its atmospheric fate, transport and transformation. Particle/gas phase distribution also controls the relative amounts of deposition (dry-wet deposition, air-water exchange).

HCHO was primarily associated with gas-phase. Particle phase ranged between 0.04 and 2% (0.45±0.44%). By comparison, Deandrade et al. (1995) reported that the average particle phase HCHO was 0.03% for air samples collected at a bus station and tunnel. Partitioning of atmospheric organic compounds between the gas and particulate phases is parameterized using the gas/particle partition coefficient, K_p (m^3 μg^{-1}) (Harner and Bidleman, 1998):

$$K_p=(C_p/C_{TSP})/C_g \quad (4.1)$$

where C_p and C_g are the organic compound concentrations in the particulate and gas phases, respectively ($\mu g\ m^{-3}$), and C_{TSP} is the concentration of total suspended particles in the air ($\mu g\ m^{-3}$). Log K_p values of semivolatile organic compounds (SOCs) (i.e. polycyclic aromatic hydrocarbons, organochlorine pesticides) range between -1.5 and -6.5 (Sofuoglu et al., 2004; Vardar et al., 2004). Even though HCHO can be classified as a volatile organic compound based on its supercooled liquid vapor pressure (log P_L=0.71 atm at 25 °C), the average log K_p value of HCHO determined in this study was -4.3±0.5, similar to those observed for SOCs.

4.1.4. Modeling the gas/particle partitioning

The octanol-air partitioning coefficient (K_{OA}) can be used to predict K_p with the assumption that the predominant distribution process is absorption (Harner and Bidleman, 1998). The relationship between K_P and K_{OA} is:

$$K_P = (f_{OM}\ MW_{OCT}\ \zeta_{OCT})\ K_{OA} / (\rho_{OCT}\ MW_{OM}\ \zeta_{OM}\ 10^{12}) \quad (4.2)$$

where f_{OM} is the fraction of organic matter phase on TSP, MW_{OCT} and MW_{OM} are the mean molecular weights of octanol and the organic matter phase (g mol^{-1}), ρ_{OCT} is the density of octanol (0.820 kg L^{-1}), ζ_{OCT} is the activity coefficient of the absorbing compound in octanol, ζ_{OM} is the activity coefficient of the compound in the organic

matter phase. With the assumptions that ζ_{OCT}/ζ_{OM} and MW_{OCT}/MW_{OM}=1, Eq. (4.2) can be written as:

$$\log K_P = \log K_{OA} + \log f_{OM} - 11.91 \quad (4.3)$$

Since log K_{OA} decreases with temperature, log K_p will also decrease with increasing temperature (Equation 4.2). Experimental log K_p values were significantly correlated with temperature ($p<0.01$) (Figure 4.6). Another parameter that could affect the gas/particle partitioning of HCHO is the relative humidity. Conditions with higher relative humidity increases the water content of aerosols and as a result the amount of HCHO dissolved in PM and K_p increases (Klippel and Warneck, 1980). The correlation between experimental log K_p values and relative humidity were also statistically significant ($p<0.01$) (Figure 4.7). However, since the temperature and relative humidity (RH) correlated negatively, it is not clear if the RH has a significant effect on K_p.

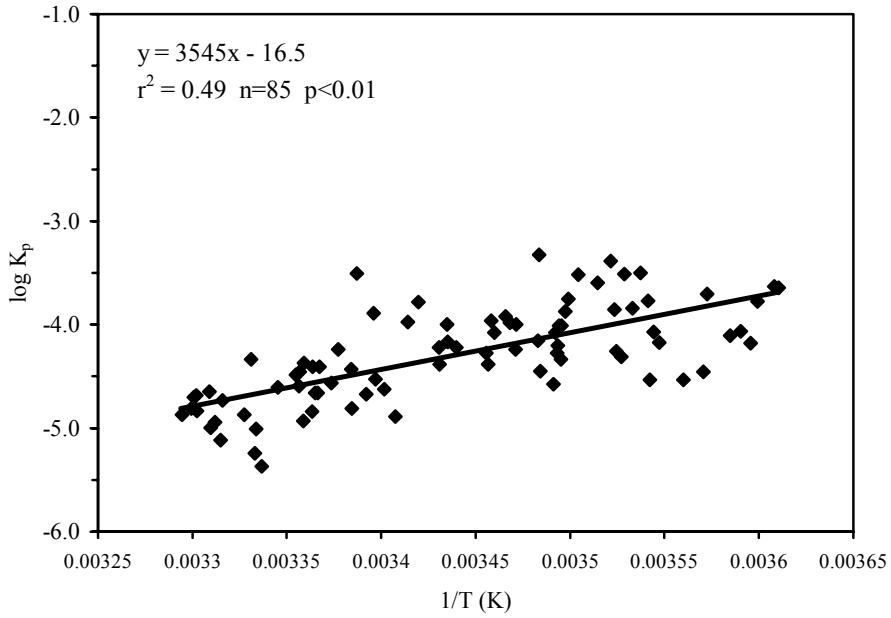

Figure 4.6 The relationship between log K_p and temperature

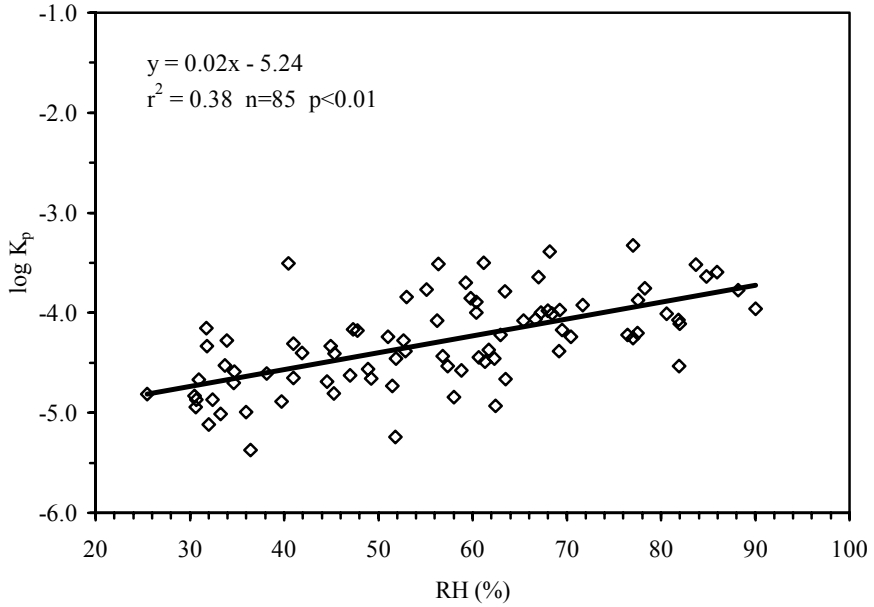

Figure 4.7 The relationship between log K_p and relative humidity

The K_P values defined in Equations (4.1) (experimental) and (4.3) (modeled) were calculated for HCHO. Measured f_{OM}, C_{TSP}, C_g, C_p and calculated K_{OA} values were used in the calculation of K_P. There were no experimental K_{OA} values available for HCHO. Therefore, the K_{OA} values were obtained as the ratio of octanol/water partition coefficient (log K_{OW} = 0.35 at 25°C) (WEB _3, 2004) to dimensionless Henry's law constant (H'). H' values as function of temperature were calculated using the experimentally determined regression parameters in this study (Section 4.3).

Figure 4.8 compares the experimentally determined and predicted log K_p values for HCHO using Equations (4.1-4.3). The K_{OA} model significantly underpredicted the experimental log K_p values. Modeled K_p values were more than five orders of magnitude smaller than the experimental ones.

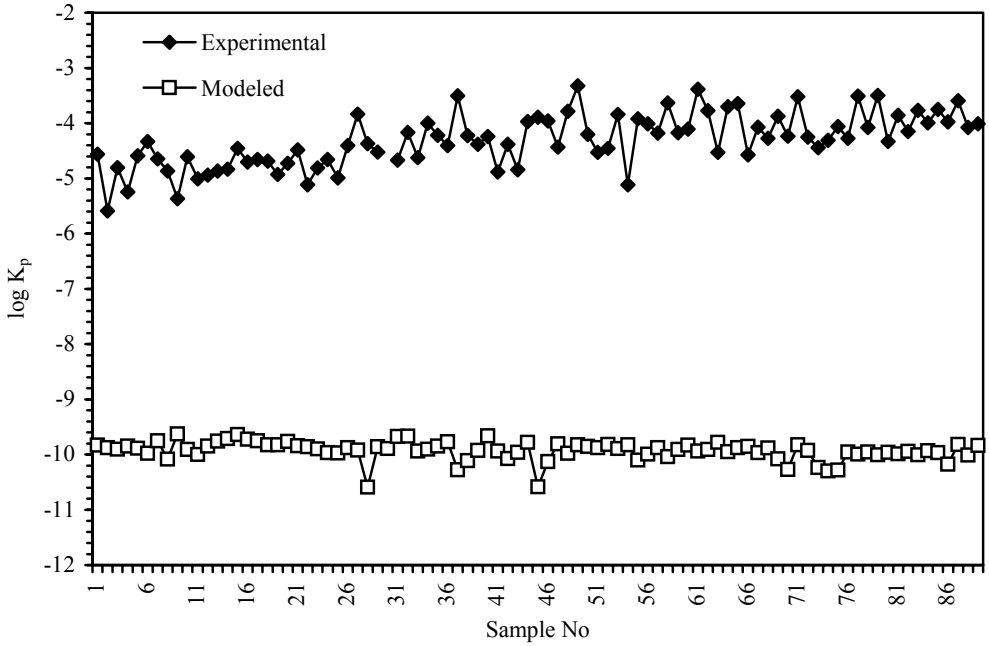

Figure 4.8 Comparison of modeled (using K_{OA} model) and experimental log K_p values for HCHO

The discrepancy between the modeled and experimental K_p values is too large to be attributed to the sampling errors or artifacts. The results suggest that the distribution of atmospheric HCHO between two phases can not be explained simply with the absorptive gas/particle partitioning theory.

Aldehydes and ketones undergo organic oxidation in the atmosphere with the accretion reactions including hydration, polymerization, hemiacetal/acetal formation, and aldol condensation (Barsanti and Pankow, 2004; Tobias and Ziemann, 2000). The term "accretion reaction" was introduced to refer to the large collection of reactions by which atmospheric organic molecules can grow in mass, especially as by combination with other organic molecules (Barsanti and Pankow, 2004). Most accretion reactions will reduce the volatility of parent organic molecules and therefore, partitioning to particulate phase becomes more favorable. It was hypothesized that such accretion reactions can occur reversibly and they could explain the measurement of anomalously

large apparent K_p values for some relatively volatile organic oxidation products (Kamens and Jaoui, 2001). It was suggested that PM-phase accretion products can revert, during the chemical analysis of the PM to the parent volatile compounds, giving the appearance of anomalously high PM-phase concentrations of parent compounds (Jang and Kamens, 2001).

The contribution of accretion products of HCHO to the observed K_p values was investigated using the K_{OA} model and their supercooled liquid vapor pressures. The K_{OA} and P_L are related through the following equation (Xiao and Wania, 2003; Shoeib and Harner, 2002):

$$K_{OA}= C_O/C_A = RT/\gamma_o V_o P_L \quad (4.4)$$

where C_O and C_A are the equilibrium concentrations (mol m^{-3}) of the solute in octanol and air respectively, R is the universal gas constant (8.314 Pa m^3 mol^{-1} K^{-1}), T is the temperature (K), γ_o is the activity coefficient in octanol, V_o is the molar volume of octanol ($1.58x10^{-4}$ m^3 mol^{-1}), and P_L is supercooled liquid vapor pressure (Pa). The activity coefficient in octanol is a measure of nonideal behavior due to interactions between solute and octanol molecules and it approaches unity for an ideal solution (Harner and Shoeib, 2002). The K_{OA} values of accretion products of HCHO were calculated with the assumption of γ_o=1. The model calculations were performed using the vapor pressures at 25°C since the temperature dependent values were not available. Predicted particulate percentages were calculated using the fraction (ϕ) of the accretion product in the particle phase (Harner and Bidleman, 1998):

$$\phi = (K_p C_{TSP})/(1+K_p C_{TSP}) \quad (4.5)$$

Supercooled liquid vapor pressures, particulate fractions and log K_p values of HCHO and its probable accretion products were presented in Table 4.1. Comparison of experimental log K_p values of HCHO and modeled ones for its two accretion products

(hydrate and hemiacetal) is shown in Figure 4.9. The agreement between experimental K_p values and those predicted for HCHO hydrate was very good (Table 4.1, Figure 4.9).For the other accretion products the model significantly overestimated or underestimated the experimental K_p values (Table 4.1).

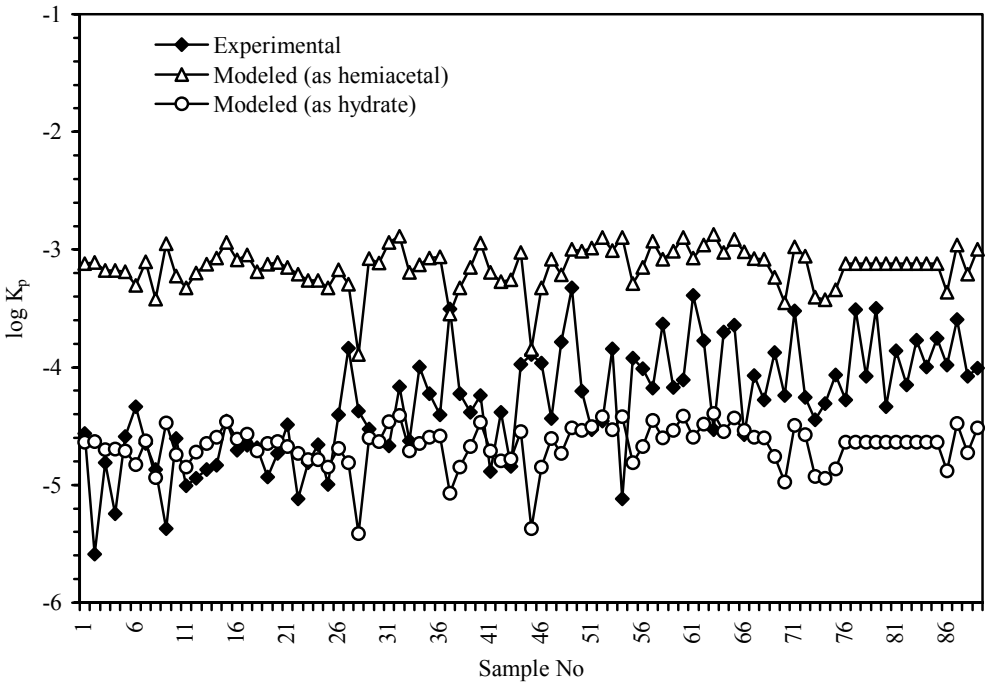

Figure 4.9 Comparison of experimental log K_p values of HCHO and modeled ones for its accretion products

Table 4.1 Supercooled liquid vapor pressures, particulate fractions and log K_p values of formaldehyde and its probable accretion products

	log P_L (atm)[a]	**Particulate phase (%)**	**log K_p**
Formaldehyde (exp.)		0.45±0.44	-4.30
Formaldehyde (modeled)	0.71	$1.01x10^{-6}$	-9.81
Hydrate	-5.35	0.15	-4.64
Hemiacetal	-6.87	4.7	-3.12
Acetal	-7.96	37.8	-2.03
β-hydroxycarbonyl	-4.08	$7.99x10^{-3}$	-5.91
α–β-unsaturated carbonyl	-0.20	$8.77x10^{-7}$	-9.87

[a] Barsanti and Pankow (2004)

A recent thermodynamic evaluation by Barsanti and Pankow (2004) has indicated that most of the accretion reactions are not thermodynamically favored in the atmosphere. However, in solution the reaction equilibrium between the HCHO and its hydrate favors the hydrate (Barsanti and Pankow, 2004). Most of the accretion reactions are reversible. Thus, equilibrium is set between formaldehyde contained in an accretion product is freed in solution. If most of the PM HCHO is present in the form of accretion product. This is important since the analytical method used in this study determines the aqueous HCHO.,. Then extraction with water the reservoir of aqueous HCHO is greatly increased and the partitioning between the bound and free HCHO is shifted in favor of free HCHO. These are consistent with the observed high K_p values in this study.

4.2. Deposition Fluxes

The results of HCHO deposition measurements will be presented in this section.

4.2.1. Particulate phase dry deposition fluxes and velocities

Particle phase HCHO fluxes measured with dry deposition plates ranged between 2-56 μg m^{-2} day^{-1} (average±SD, 17±12 μg m^{-2} day^{-1}) (Figure 4.10). There are no previous measurements or estimations reported in the literature for dry deposition of HCHO. Therefore, measured HCHO fluxes were compared to the fluxes of semivolatile organic compounds like PAHs. Measured dry deposition fluxes of HCHO were within the ranges previously measured for PAHS using similar techniques at different sites around the world (Table 2.3).

Figure 4.11 shows the particulate phase dry deposition velocities for HCHO calculated using the particulate fluxes measured with dry deposition plates and ambient particulate concentrations. The dry deposition velocity for HCHO ranged from 0.1 to 9.6 cm s^{-1} with an average of 1.4±1.4 cm/s.

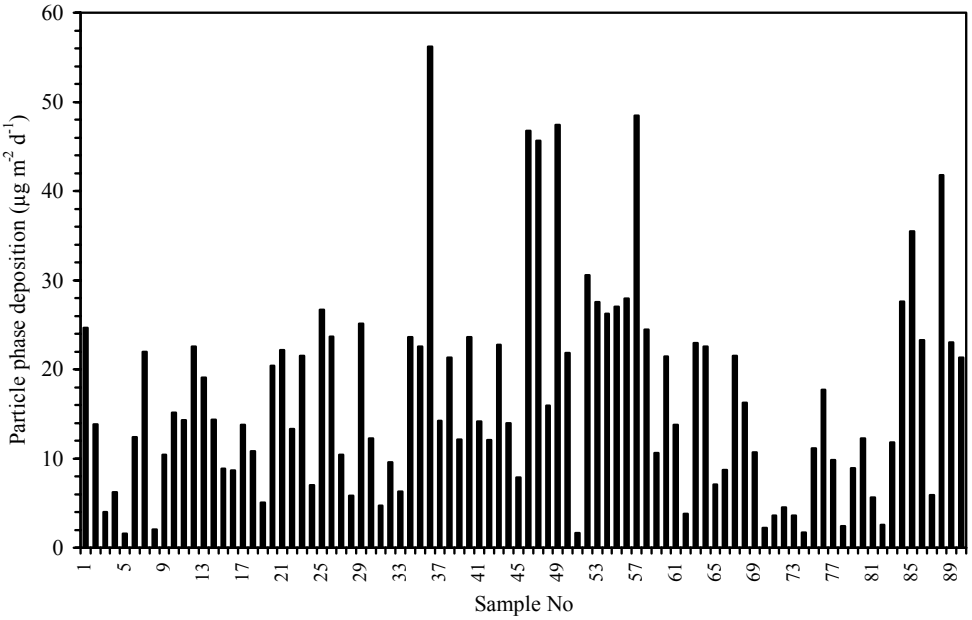

Figure 4.10 Variation of particle phase formaldehyde deposition flux during the sampling program

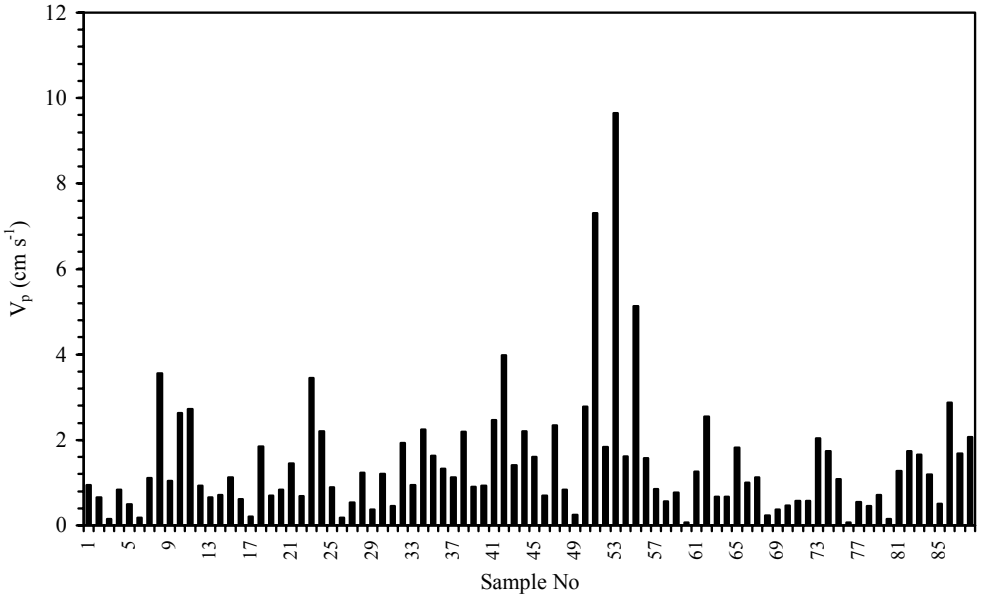

Figure 4.11 Overall dry deposition velocities for particulate formaldehyde

Reported values for the particle phase dry deposition velocities of different pollutants are summarized in Table 4.2. The dry deposition velocity calculated in this study for HCHO agrees well with the previously reported values determined using similar techniques (dry deposition plates).

Table 4.2 Dry Deposition Velocities for Formaldehyde and Other Compounds Associated with the Particles

Species [a]	V_p (cm s^{-1})	Method	Reference
Sulfate	0-3.0	Modeled (3.8 μm particles)	Zhang et al. (2001)
Sulfate	0-4.0	Gradient	Wyers and Duyzer (1997)
Sulfate	0.10	Modeled	Morales et al. (1998)
Sulfate	0.10-0.30	Modeled	Zeller et al. (1997a)
Sulfate	6.3±3.9	Dry deposition plates	Odabasi and Bagiroz (2002)
Trace elements	0.6-6.2	Dry deposition plates	Odabasi et al. (2002)
Trace elements	2.0-12.0	Dry deposition plates	Yi et al. (2001)
OCP	5.0 ± 2.0	Dry deposition plates	Cakan (1999)
PCB	5.0	Dry deposition plates	Holsen et al. (1991)
PCB	5.2±2.9	Dry deposition plates	Tasdemir et al. (2004)
PCB	4.4-7.2	Dry deposition plates	Franz et al. (1998)
PAH	0.4-3.7	Dry deposition plates	Franz et al. (1998)
PAH	6.7±2.8	Dry deposition plates	Odabasi et al. (1999)
PAH	4.5±3.1	Dry deposition plates	Vardar et al., 2002
Formaldehyde	1.4±1.4	Dry deposition plates	This study

[a] Polychlorinated biphenyls (PCB), organochlorine pesticides (OCP), polycyclic aromatic hydrocarbons (PAH)

4.2.2. Wet Deposition

Formaldehyde concentration was measured in 27 rain samples collected at the sampling site. Rainwater HCHO concentrations ranged between 10-304 μg l^{-1} with an average value of 94±61 μg l^{-1} (Figure 4.12). Measured rainwater HCHO concentrations were within the range reported in the literature (Table 2.4).

Rainout and washout are the two major mechanisms that transfer pollutants into rainwater. Rainout includes processes that take place in clouds (i.e., nucleation, condensation, gas dissolution). Washout is the process that scavenges air pollutants between the cloud and the Earth's surface (Pena et al., 2002). In previous studies (Largiuni et al., 2002; Pena et al., 2002; Kieber et al., 1999) no or positive correlation was found between rainfall and HCHO concentrations, suggesting continuous supply or in situ photochemical production in aqueous phase during rain events. However, Sakugawa et al. (1993) found that rainwater HCHO concentrations were strongly dependent on precipitation amount and the concentration decreased with increasing precipitation volume, suggesting that washout dominated rainwater concentrations. The relationship between the amount of precipitation and HCHO concentration was investigated using linear regression analysis in the present study. The correlation between rainwater HCHO concentration and precipitation volume was statistically significant (r^2=0.43, $p<0.01$). The rainwater concentration decreased with precipitation volume indicating that HCHO concentrations were mostly controlled by washout. Kieber et al. (1999) have suggested that if gas-phase HCHO concentrations are high, washout may dominate rainwater concentrations relative to HCHO contributed from continuous supply during rain events. This may explain why a correlation between precipitation amount and HCHO concentrations is observed at some locations and not others (Kieber et al., 1999).

Using the rainwater concentrations and rainfall amounts the annual formaldehyde wet deposition was calculated as 30155 μg m^{-2} yr^{-1} (Table 4.3). This was comparable to the

wet deposition fluxes reported previously for Los Angeles, USA and Heraklion, Greece (Sakugawa et al. 1993; Kieber et al. 1999).

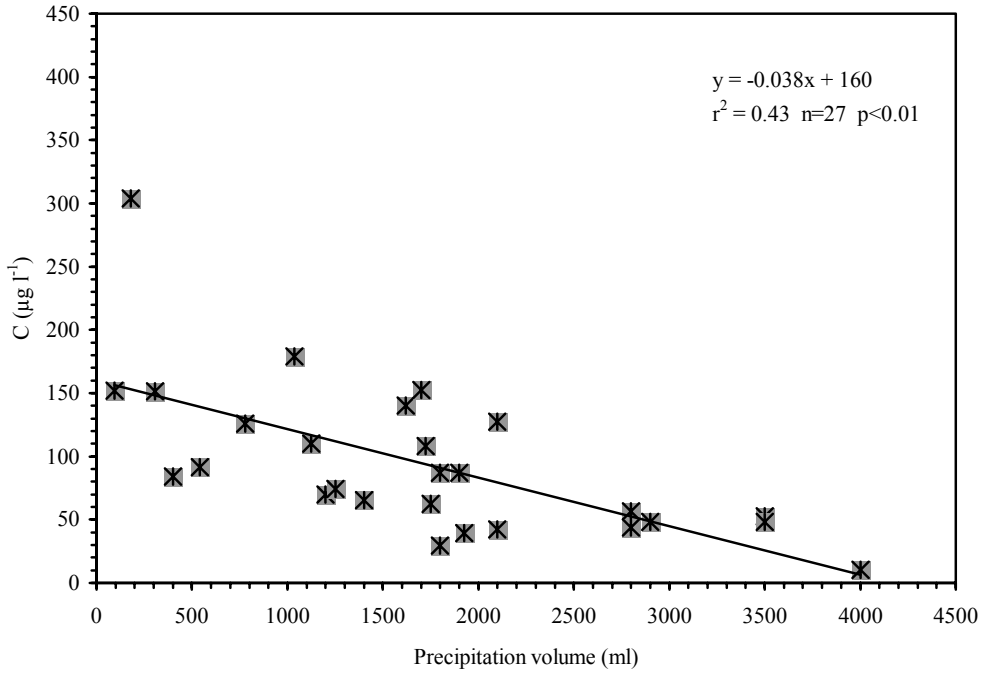

Figure 4.12 Relationship between the rainwater HCHO concentrations and rain water volume

Table 4.3 Comparison of Wet Deposition Fluxes (µg m^{-2} yr^{-1}) of HCHO with Other Studies

Location	Period	Flux	Reference
Los Angeles, USA	1985-1991	34000	Sakugawa et al. (1993)
Wilmington, NC	1996-1998	138000	Kieber et al. (1999)
Heraklion, Greece	1999-2000	45000	Economou and Mihalopoulos (2002)
Izmir, Turkey	2003-2004	30155	This study

Figure 4.13 shows the variation of monthly dry and wet deposition fluxes. During the rainy season (October through April) total deposition (wet+dry) is dominated by wet deposition while dry deposition is the dominating mechanism during the dry season. The annual dry deposition flux was determined as 6105 μg m^{-2} yr^{-1} using the measured dry deposition fluxes. The annual HCHO total deposition (wet+dry) was calculated as 36260 μg m^{-2} yr^{-1} and it was dominated by wet deposition (83.2%).

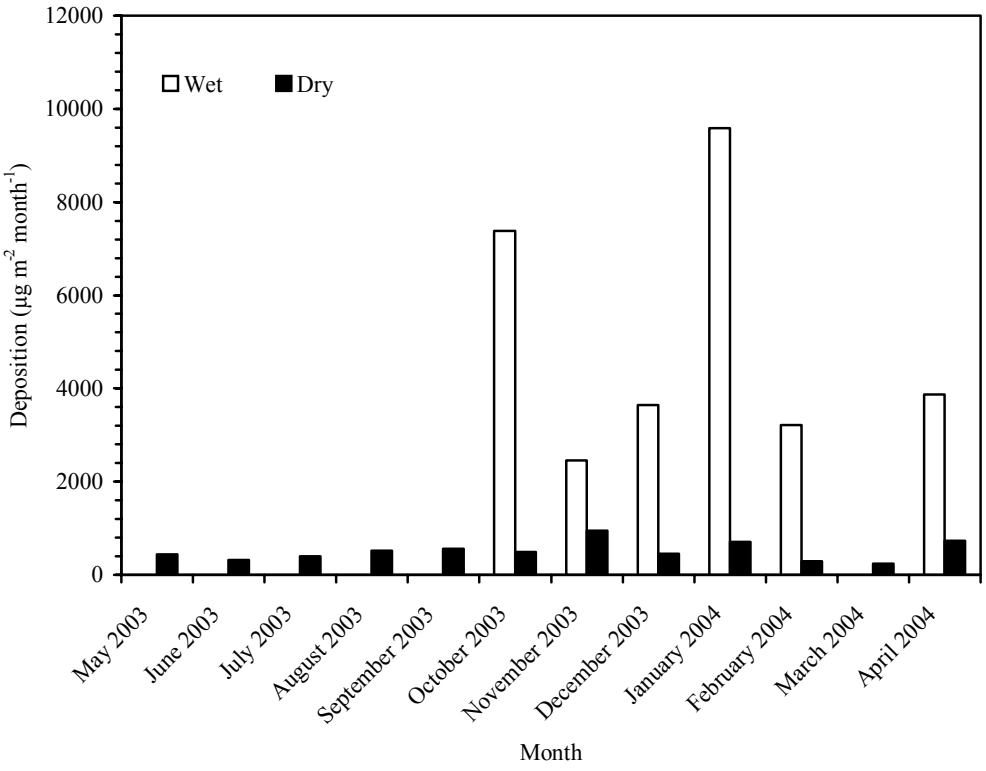

Figure 4.13 Comparison of dry and wet deposition of formaldehyde

4.3. Air-water exchange

The results of HCHO air-water exchange flux measurements conducted in the field and in the laboratory will be presented in this section.

4.3.1. Field Studies

4.3.1.1 Gas Phase Fluxes

Gas phase dry deposition fluxes were calculated by subtracting the particulate phase fluxes measured with dry deposition plate from the total (gas+particle) fluxes measured with the WSS. Recent studies indicated that particulate dry deposition flux of some organic and inorganic species (PAHs, lead, and calcium) was statistically the same to the dry deposition plate and WSS indicating that both of these surrogate surfaces have similar characteristics for atmospheric particle collection (Odabasi et al., 1999; Yi et al., 1997). The range for gas phase HCHO flux was 273-5404 μg m^{-2} day^{-1} and the average value was 1200±888 μg m^{-2} day^{-1} (Figure 4.14). The average total (gas+particle) flux measured with the WSS was 1219±886 μg m^{-2} day^{-1} and it was dominated by gas phase flux. Gas phase flux accounted for 98.6% of the total (gas+particle) flux. Daytime fluxes (1439±1032 μg m^{-2} day^{-1}) were generally higher than the nighttime fluxes (849±433 μg m^{-2} day^{-1}) probably due to higher ambient concentrations. The annual gas phase flux to the WSS ($4.38x10^5$ μg m^{-2} yr^{-1}) was 12 times higher than the total (wet+dry) deposition flux. The only previously reported value for HCHO gas phase deposition to the water surfaces is 197 μg m^{-2} day^{-1} (Zhou and Mopper, 1997) and corresponded to a relatively lower ambient concentration (0.5 μg m^{-3}). This flux is similar to the minimum value measured in this study.

4.3.1.2 Gas Phase Overall Mass Transfer Coefficients

The HCHO gas phase overall mass transfer coefficients were calculated from experimental data as:

$$K_g=F_g/(C_g - C_wH/RT) \quad (4.6)$$

where C_w and C_g are the water and air concentrations of HCHO (μg m^{-3}), H is the Henry's law constant (L atm mol^{-1}), R is the universal gas constant (0.08205 L atm mol^{-1} K^{-1}), and T is temperature at the air-water interface (K). In the calculation of K_g it was assumed that the HCHO concentration in water (C_w) was zero since HCHO is hydrated to form $CH(OH)_2$ immediately upon transfer to water.

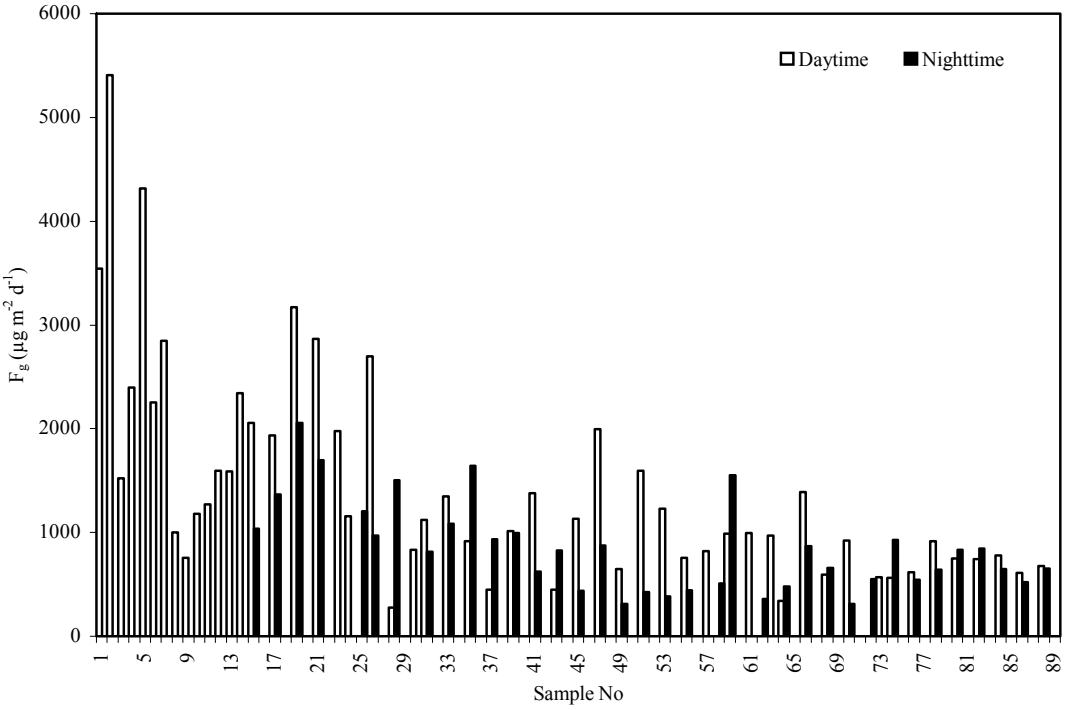

Figure 4.14 Variation of gas phase fluxes. Note that the first 14 samples are 24 h samples

The calculated K_g values ranged from 0.07 to 0.59 cm s^{-1} with an overall average of 0.25±0.12 cm s^{-1}. The average K_g calculated from daytime samples (0.21±0.10 cm s^{-1}) was lower than the average value for nighttime samples (0.29±0.14 cm s^{-1}). The relationship between the gas phase HCHO fluxes and ambient concentrations is shown in Figure 4.15. Gas phase fluxes and ambient concentrations correlated well (r^2= 0.77, $p<0.01$).

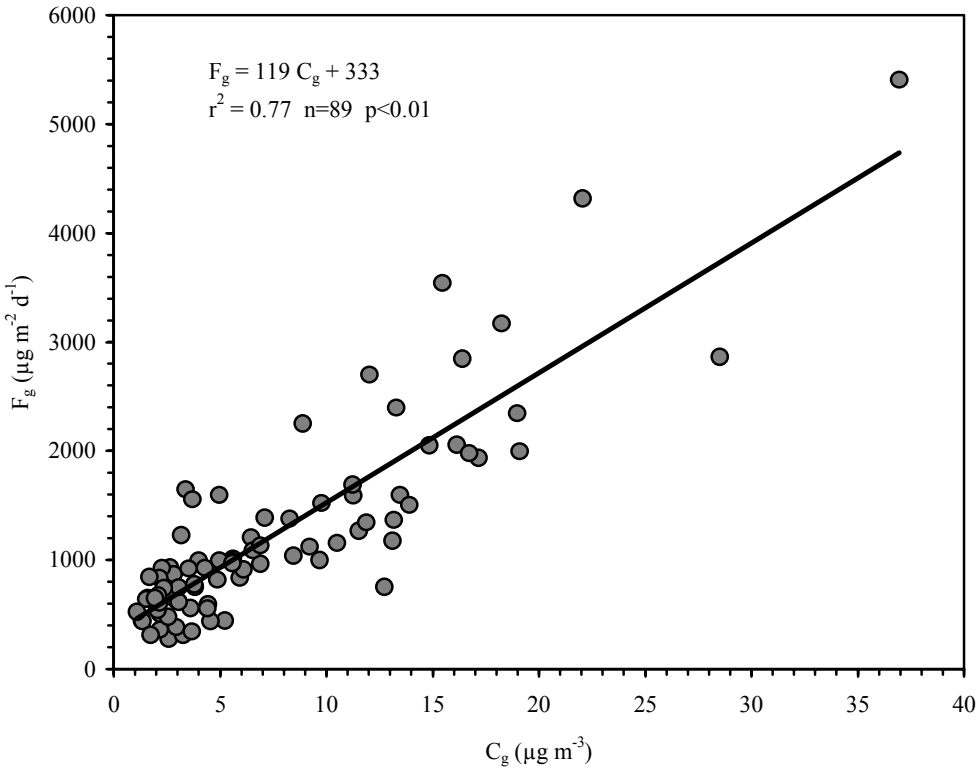

Figure 4.15 Relationship between HCHO flux and ambient concentration (Field study)

The slope of the linear regression line is the best-fit gas phase overall mass transfer coefficient (K_g) with units of m d^{-1}. K_g obtained from linear regression was 0.14 cm s^{-1} and reasonably agreed with the average K_g value of 0.25 cm s^{-1}.

4.3.2. Laboratory Studies

The results of HCHO air-water exchange flux and concurrent gas-phase concentration measurements conducted in the laboratory will be presented in this section.

4.3.2.1 Gas Phase Overall Mass Transfer Coefficients

The calculated K_g values ranged from 0.16 to 0.91 cm s^{-1} with an overall average of 0.60±0.22 cm s^{-1}. The average K_g calculated from indoor experiments was 2.4 times higher than the average value calculated from field samples (0.25±0.12 cm s^{-1}).

The relationship between the gas phase HCHO fluxes and indoor concentrations is shown in Figure 4.16. The correlation between the gas phase fluxes and indoor concentrations was very good (r^2= 0.94). The slope of the linear regression line is the best-fit gas phase overall mass transfer coefficient (K_g) with units of m d^{-1}. K_g obtained from linear regression was 0.71 cm s^{-1} and agreed well with the average K_g value of 0.60 cm s^{-1}.

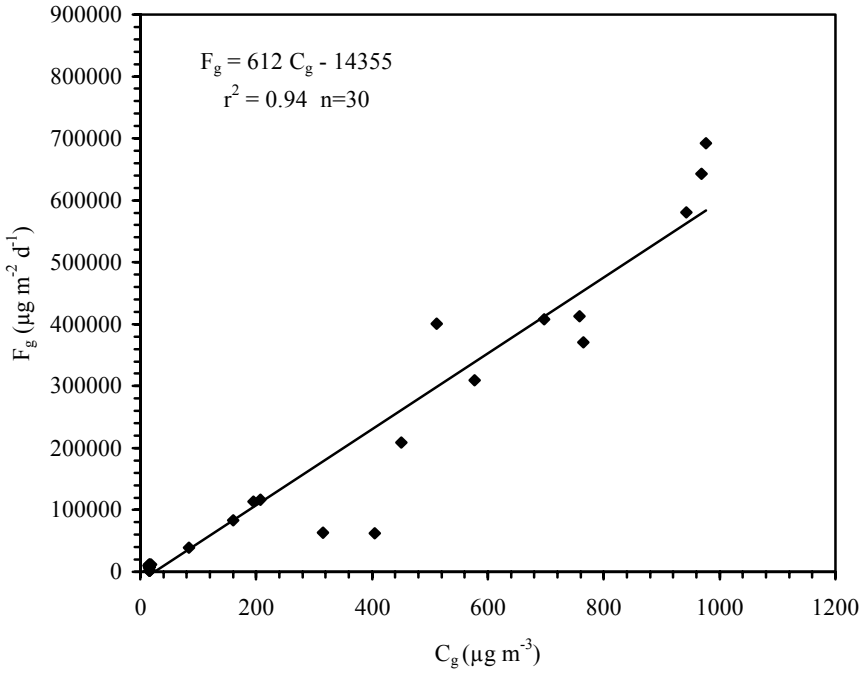

Figure 4.16 Relationship between HCHO flux and indoor air concentration

4.3.3. Modeling the Gas Phase Overall Mass Transfer Coefficients

Two different two-film models, one previously developed based on experiments performed with the WSS (for nonreactive species, Model I) and, one previously published (for reactive species, Model II), were used to calculate modeled overall mass transfer coefficients for HCHO. Several equations (equation 2.7 through equation 2.26) were used to calculate modeled K_g values as described in Section 2.5 (Table 4.4).

4.3.3.1 Determination of Henry's law constant for formaldehyde

Henry's law constant of HCHO has a crucial importance in determining its air-water exchange. The previously determined Henry's law constant of HCHO by Betterton and Hoffmann (1988) contained some inconsistency related to its temperature-dependence. Therefore, it has also been determined in this study at six temperatures (50, 40, 30, 20, 10, and 5°C) using a bubble column technique. Three replicate experiments were conducted at each temperature. The H^* values were strongly correlated to inverse of temperature (1/T, K) (Figure 4.17) and the following relationship was obtained:

$$\ln H^* = (1641.3/T) - 3.089 \qquad (4.7)$$

Figure 4.18 compares results of this study to those reported in the literature. H^* was 1.85×10^{-4} L atm mol^{-1} (at 25ºC) and it was in reasonable agreement with previously reported values of 3.37×10^{-4}, 3.16×10^{-4}, and 1.0×10^{-4} L atm mol^{-1} (Betterton and Hoffmann, 1988; Dong and Dasgupta, 1986; Kim et al., 2000).

Table 4.4 The Summary of Models Used to Calculate K_g (cm s^{-1})

Model I (no enhancement)	Ref.	Model II (enhancement due to reaction)	Ref.
$k_g = D_a^{0.5} (0.98\ u_{10} + 1.26)$	(1)	$k_g = D_a^{0.5} (0.98\ u_{10} + 1.26)$	(1)
$D_a = 10^{-3}\{T^{1.75}[(1/m_{air}) + (1/m)]^{1/2}/P[V_{air}^{1/3} + V^{1/3}]^2\}$	(2, 4)	$D_a = 10^{-3}\{T^{1.75}[(1/m_{air}) + (1/m)]^{1/2}/P[V_{air}^{1/3} + V^{1/3}]^2\}$	(2, 4)
$k_{w(O2)} = 1.62x10^{-3} + 2.23x10^{-4}\ u_{10} + 1.66x10^{-4}\ u_{10}^2$	(3)	$k_{w(O2)} = 1.62x10^{-3} + 2.23x10^{-4}\ u_{10} + 1.66x10^{-4}\ u_{10}^2$	(3)
$D_w = 13.26x10^{-5}/(\mu^{1.14}.V^{0.589})$	(4)	$D_w = 13.26x10^{-5}/(\mu^{1.14}.V^{0.589})$	(4)
$k_{w(compound)}$ (cm s^{-1}) = $k_{w(O2)}$ $[D_{w(compound)}/D_{w(O2)}]^{0.5}$	(4)	$k_{w(compound)}$ (cm s^{-1}) = $k_{w(O2)}$ $[D_{w(compound)}/D_{w(O2)}]^{0.5}$	(4)
$\ln H^* = (1641.3/T) - 3.089$	(5)	$\ln H^* = (1641.3/T) - 3.089$	(5)
K_h=exp[(3769/T)-5.494]	(6)	K_h=exp[(3769/T)-5.494]	(6)
$H = H^* (1+K_h)$	(7)	$H = H^* (1+K_h)$	(7)
$1/K_g = (1/k_g) + (H/RTk_w)$	(7)	k_h=2.05x10^5 exp(-2936/T)	(6)
		k_d=4.96x10^7 exp(-6705/T)	(8)
		$t_w = (D_w/k_w^2)$	(7)
		t_r=1/(k_h+k_d)	(7)
		$q = (2t_w/t_r)^{1/2}$	(7)
		$\Psi = (K_h + 1)/[1 + (K_h/q).\tanh q]$	(7)
		$1/K_{g(enhanced)}$=(1/k_g)+(H/RT$k_w\Psi$)	(7)

(1) Shahin et al. (2002)

(2) Lyman et al. (1993)

(3) Odabasi et al. (2001)

(4) Schwarzenbach et al. (1993)

(5) This study

(6) Winkelman et al. (2002)

(7) Schwarzenbach et al. (2003)

(8)Winkelman et al. (2000)

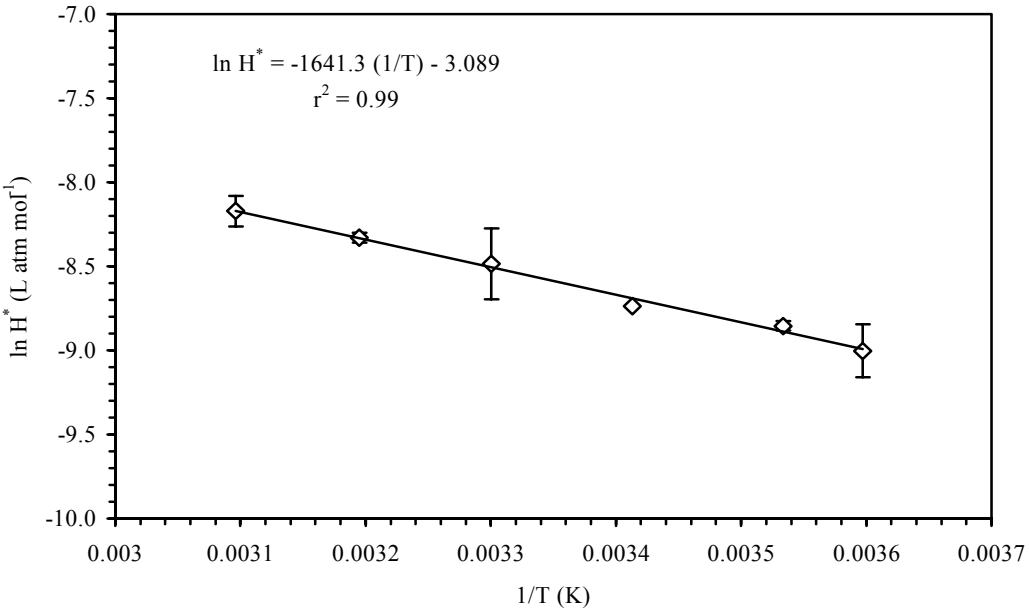

Figure 4.17 Variation of H^* with temperature. Error bars are 1 SD (n=3)

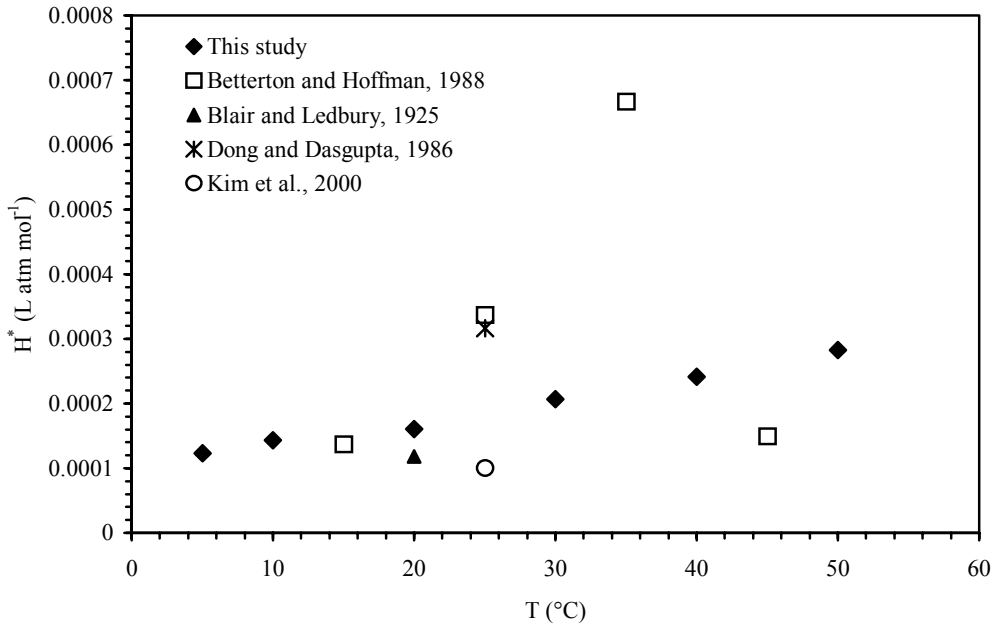

Figure 4.18 Comparison of H* determined in this study with literature values

4.3.3.2 Examination of modeling results for laboratory studies

The measured K_g values for HCHO were compared to the predictions of two different models, one previously developed based on experiments performed with the WSS (for nonreactive species, no enhancement) and, one previously published (for reactive species, considering enhancement due to chemical reaction) (Figure 4.19). Gas phase mass transfer velocities (K_g) and wind speed (U) correlated well ($y=0.16x + 0.33$, $r^2= 0.71$).

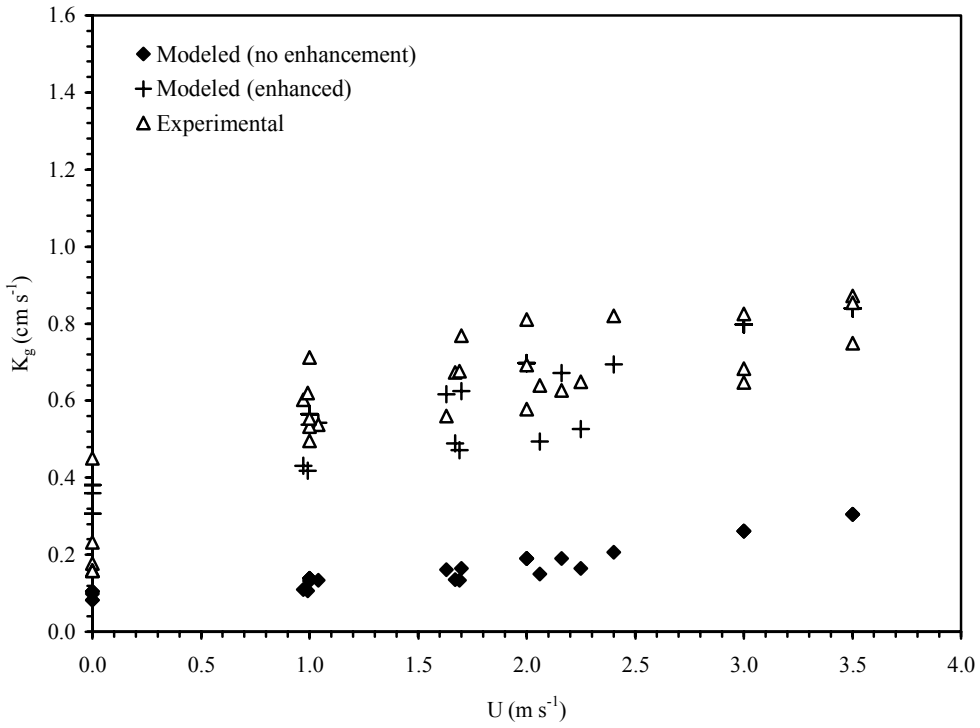

Figure 4.19 Variation of experimental and modeled K_g values obtained in laboratory studies with wind speed.

Model I examination

The measured K_g values for HCHO were compared with the predictions of the Model I (no enhancement) (Figure 4.20). The linear model including standard errors (at the 95% confidence level) of the slope and the intercept for HCHO is:

$$\textit{Measured } K_g = (2.23 \pm 0.42)(\textit{Modeled } K_g) + (0.2 \pm 0.08) \qquad (4.8)$$

The statistically significant relationship (r^2=0.50, $p<0.01$) between the measured and modeled K_g indicates that the wind speed is a useful parameter for the prediction of the mass transfer coefficient in the boundary layer over the WSS.

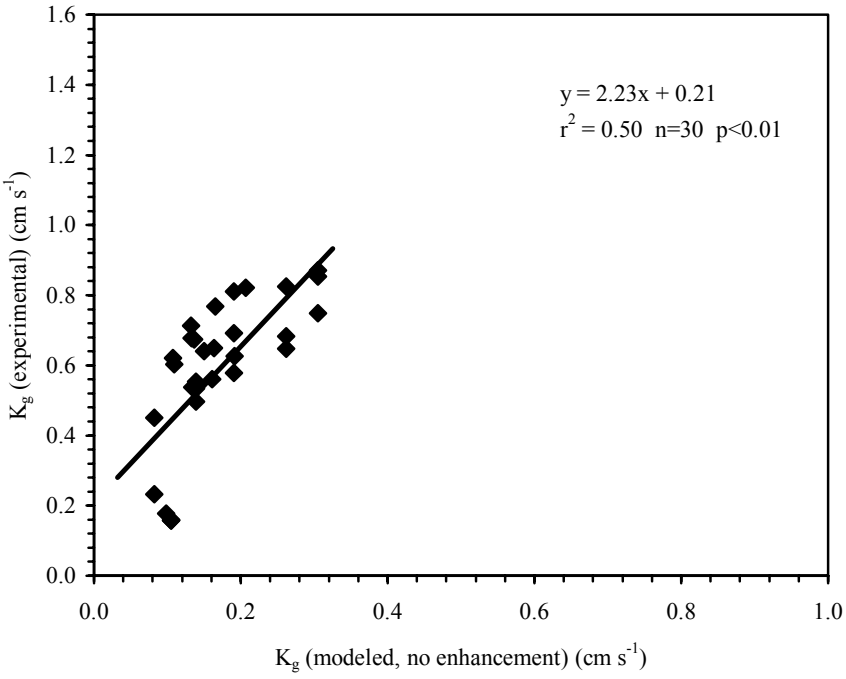

Figure 4.20 Comparison of experimental and modeled (not enhanced) K_g values obtained in laboratory studies

However, slope of the best-fit model (2.2) larger than 1 indicates that the Model I significantly underestimates the mass transfer coefficient in the boundary layer.

Model II examination

The measured K_g values for HCHO were compared to the predictions of the Model II (Figure 4.21). The linear model including standard errors (at the 95% confidence level) of the slope and the intercept for HCHO is:

$$\textit{Measured } K_g = (0.98\pm0.15)(\textit{Modeled } K_g) + (0.02\pm0.09) \qquad (4.9)$$

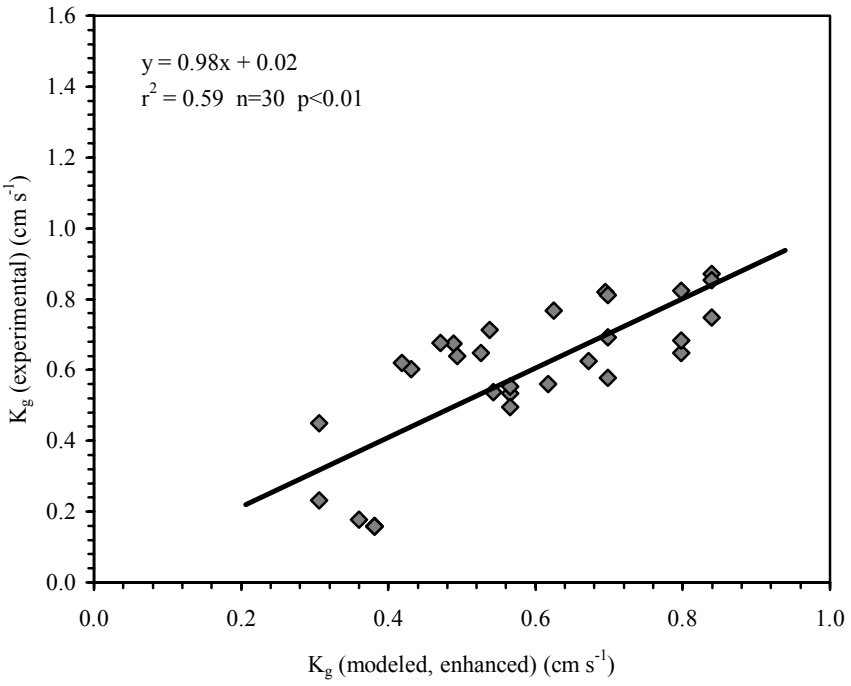

Figure 4.21 Comparison of experimental and modeled (enhanced) K_g values obtained in laboratory studies

The statistically significant relationship (r^2=0.59, $p<0.01$) between the measured and modeled K_g, the slope of the regression line (0.98) close to 1.0 and the intercept close to zero indicates an excellent agreement between predicted and measured values.

Comparison of overall mass transfer coefficients of formaldehyde predicted by two models and those determined experimentally indicated that under the laboratory conditions of this study, there was a flux enhancement of HCHO mass transfer due to chemical reaction and it ranged between 2.8 and 4.1 (average±SD, 3.6±0.4) times.

4.3.3.3 Examination of modeling results for field studies

The measured K_g values for HCHO were compared to the predictions of two different models, one previously developed based on experiments performed with the WSS (for nonreactive species, no enhancement, Model I) and, one previously published (for reactive species, considering enhancement due to chemical reaction, Model II) (Figure 4.22). Regression analysis indicated that there is not a statistically significant linear relationship ($p>0.1$) between the measured and modeled K_g values. The average measured K_g (0.25 cm s^{-1}) was significantly lower than the average predictions of Model I (0.44 cm s^{-1}) and the Model II (0.90 cm s^{-1}). Measured and modeled overall mass transfer coefficients were also compared by calculating the measured/modeled ratios. For a good prediction this ratio should be close to unity. The average measured to modeled ratio for the Model I was 0.92±0.90. Even though the ratio is close to 1.0 this resulted from the averaging ratios much higher or lower than 1.0, as can be seen from the large standard deviation. The average measured to modeled ratio for the Model II was 0.33±0.25, suggesting that the model significantly overestimated the experimental K_g values.

Figure 4.22 also shows the relationship between the experimental or modeled K_g values and the wind speed. Measured K_g values were not correlated to wind speed. However, although there is a reasonable amount of scatter in the data, modeled values

were correlated to wind speed indicating that the wind speed is an important parameter in predicting mass transfer coefficients of air pollutants. Comparison of two models used in prediction of overall mass transfer coefficients of formaldehyde indicated that under the meteorological conditions of this study, the enhancement of HCHO mass transfer due to chemical reaction ranges between 1.1 and 4.0 (average±SD, 2.5±0.9) times.

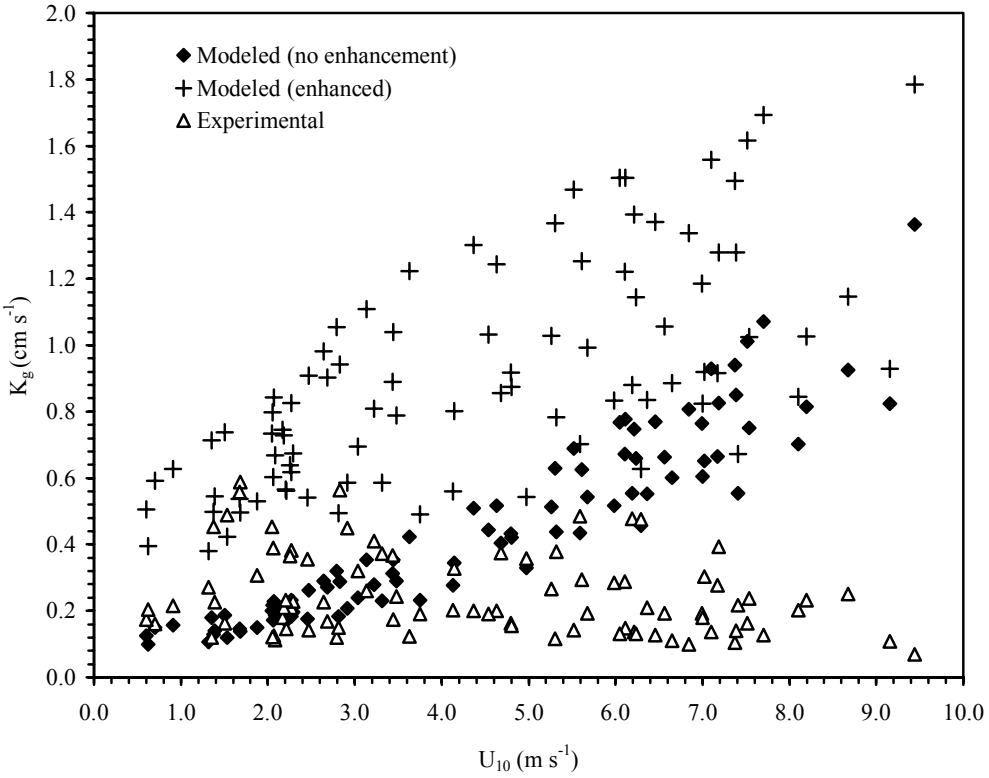

Figure 4.22 Comparison of experimental and modeled K_g values obtained in field studies

The model used in this study to predict the mass transfer coefficients of HCHO was developed based on experiments conducted with the WSS. Recently, this model was successfully used to predict K_g values for various organic and inorganic pollutants (PAHs, NH_3, HNO_3, SO_2) to the WSS (Odabasi et al., 2001; Shahin et al., 2002). As shown in the present study, the model was also very successful in predicting the K_g

values measured under laboratory conditions when flux enhancement due to chemical reaction is included in the model.

This discrepancy between the mass transfer coefficients measured in the field and those modeled may be due to the following reasons: 1) the assumption of the HCHO concentration in water (C_w) was zero in calculation of K_g does not hold, 2) the interference of sulfite and bisulfite affected the measurement of HCHO in the field samples, 3) losses of deposited HCHO from the WSS by chemical or photochemical degradation.

The assumption of the HCHO concentration in water (C_w) was zero in calculation of K_g was checked using the equation 4.6, the measured water (C_w) and air (C_g) concentrations, and temperature adjusted Henry's law constant of HCHO. In this case, it was assumed that the variation of C_w during sampling was linear:

$$C_w=(C_{wi}+C_{wf})/2 \quad (4.10)$$

where C_{wi} and C_{wf} are the initial and final HCHO concentrations in water. Since $C_{wi}=0$, Equation 4.7 is reduced to:

$$C_w=C_{wf}/2 \quad (4.11)$$

The average K_g calculated using the Equations 4.6 and 4.8 was 0.29±0.16 cm s^{-1}, only 15% higher than the average K_g calculated with the assumption of zero HCHO concentration in water. This calculation indicated that as initially assumed, the HCHO concentration in water was small and did not significantly limit the air-water exchange process by decreasing the fugacity difference.

Sulfite (SO_3^{2-}) and bisulfite (HSO_3^-) react with formaldehyde to form hydroxymethane sulphonate (HMS^-, $CH_2(OH)SO_3^-$) (Winkelman et al., 2000; Kieber et al., 1999):

$$CH_2(OH)_2 \rightarrow CH_2O + H_2O \quad (4.12)$$

$$CH_2O + SO_3^{2-} \rightarrow CH_2(O^-)SO_3^- \quad (4.13)$$

$$CH_2(O^-)SO_3^- + H^+ \rightarrow CH_2(OH)SO_3^- \quad (4.14)$$

$$CH_2(OH)_2 + HSO_3^- \rightarrow CH_2(OH)SO_3^- + H_2O \quad (4.15)$$

When formaldehyde is removed during the DDL development in analysis, the HMS^- decomposes. For small concentrations of sulfite the decomposition is fast enough and the analysis remains unaffected. A noticeable reduction of DDL after a reaction time of 30 min was reported for sulfite concentrations greater than10^{-5} M (Klippel and Warneck, 1980). The HMS^- can be destroyed by oxidation of sulfite with iodine. Thus, the interference with DDL formation is removed.

The interference of sulfite with HCHO analysis was also investigated in this study by spiking HCHO containing solutions (0.1, 0.3, 0.5, and 1.0 μg ml^{-1}) with $3.3x10^{-5}$, $9.9x10^{-5}$, $1.7x10^{-4}$, $3.3x10^{-4}$, $1.7x10^{-3}$ M Na_2SO_3 (n=20). Having the same concentrations, another series of solutions was prepared and treated with iodine solution (n=20). Both series of solutions were analyzed for formaldehyde. Results of this experiment indicated that HCHO loss during the analysis was dependent on sulfite concentration rather than HCHO concentration. The loss of HCHO ranged from 5% for $3.3x10^{-5}$ M sulfite to 88% for $1.7x10^{-3}$ M sulfite. The increase of HCHO loss was exponential. The sulfite spiked samples have shown no significant loss when they were treated with iodine solution.

The interference of sulfite/bisulfite causes an underestimation in HCHO concentration. The water concentration of sulfite in WSS and in the impinger used for air sampling can be different resulting in different degrees of interference in air and deposition sampling. The transfer of sulfite into impinger is limited with the volume of air sampled while the sulfite transfer into the WSS is controlled by the deposition surface and sampling time. Calculations indicated that under the sampling conditions of this study the sulfite or bisulfite concentration in the deposition sample can be several times higher than the concentration in air sample.

The possible interference of sulfite with HCHO analysis was checked by treating some samples (n=18) with iodine solution during the analysis. The results are presented in Figure 4.23.

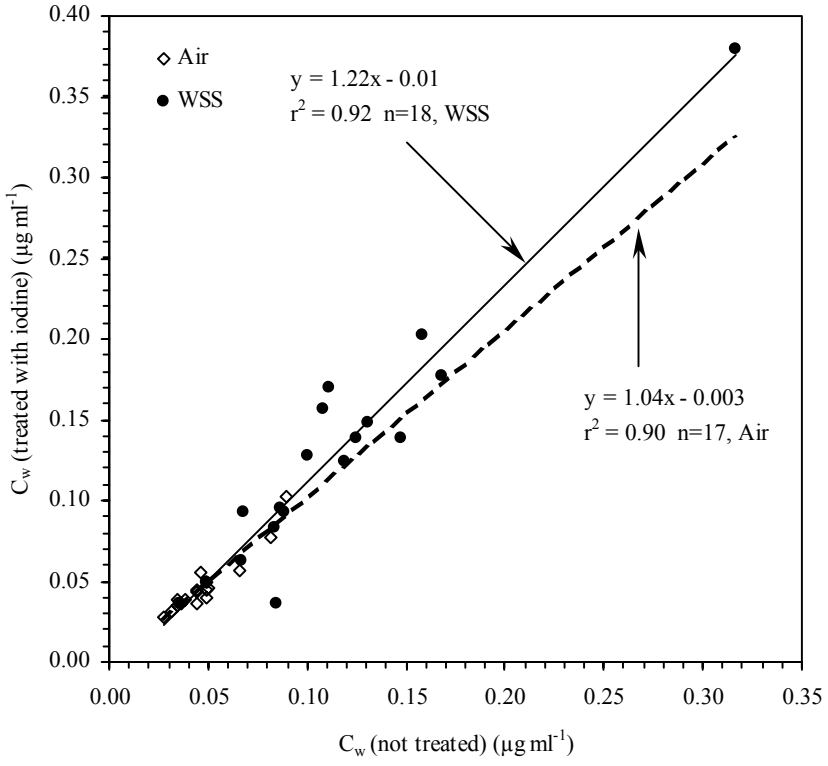

Figure 4.23 Comparison of iodine treated and not treated samples

Concentrations of treated and not treated samples correlated well for both WSS and air samples. For air samples the slope of the regression line (1.04) was close to 1.0 indicating that sulfite/bisulfite interference was not significant for air samples. However, for WSS samples the slope of the regression line (1.22) was higher than 1.0 indicating that on the average sulfite/bisulfite interference resulted in approximately 20% underestimation in measured HCHO fluxes.

Another possible explanation for the discrepancy between the measured and modeled mass transfer coefficients is the loss of deposited HCHO from the WSS by chemical or photochemical degradation. Formaldehyde is highly soluble in water and reacts with water to form $CH_2(OH)_2$:

$$HCHO + H_2O \underset{k_d}{\overset{k_h}{\rightleftharpoons}} CH_2(OH)_2 \qquad (4.16)$$

This hydrated formaldehyde does not absorb solar radiation and therefore the lifetime of HCHO in water is longer than in the gas phase (Sanhueza et al., 1991). The more probable reaction of HCHO in water is with the hydroxyl radical ($OH^{\cdot}$) (Kieber et al., 1999; Sanhueza et al., 1991):

$$CH_2(OH)_2 + OH^{\cdot} \rightarrow {}^{\cdot}CH(OH)_2 + H_2O \qquad (4.17)$$

$${}^{\cdot}CH(OH)_2 + O_2 \rightarrow HCOOH_{(aq)} + HO_2^{\cdot} \qquad (4.18)$$

The aqueous formic acid ($HCOOH_{(aq)}$) can evaporate to the gas phase or dissociate:

$$HCOOH_{(aq)} \leftrightarrow HCOOH_{(g)} \qquad (4.19)$$

$$HCOOH_{(aq)} \leftrightarrow H^+ + HCOO^- \qquad (4.20)$$

$HCOO^-$ can be further oxidized by hydroxyl radical (Sanhueza et al., 1991):

$$HCOO^- + OH^- \xrightarrow[O_2]{H^+} H_2O + CO_2 + H_2O \quad (4.21)$$

It was suggested that in-cloud oxidation of formaldehyde plays an important role in controlling the concentration of formic acid in tropical rains (Sanhueza et al., 1991). It was calculated that the steady state between HCHO and $HCOO^-$ is established within a few minutes with a molar ratio of 1.0 for a pH range of 5-7 (Economou and Mihalopoulos, 2002; Sanhueza et al., 1991). The correlation between HCHO and formic acid and their observed ratio near unity in the rainwater supports this hypothesis. However, more recent estimates suggest that HCHO/$HCOO^-$ ratio should be 0.25 (Economou and Mihalopoulos, 2002). Therefore, it is not clear that if the observed correlations between HCHO and formic acid indicate in-cloud production of $HCOO^-$ from HCHO. However, this proposed reaction mechanism is important. If it is favorable in rainwater, it is possible that it could take place on the WSS under atmospheric conditions and may be responsible in part for the low fluxes and K_g values observed in the field sampling of this study.

The experimental and modeling work conducted in laboratory in this study indicated that wind speed is an important parameter in determining K_g. However, field measured K_g values for HCHO were not correlated with wind speed. The average wind speeds for daytime and nighttime samples were 5.0 and 3.5 m s^{-1}, respectively. However, the average daytime and nighttime K_g values were 0.21 and 0.29 cm s^{-1}. Even though the wind speed was 1.4 times lower, the average K_g was approximately 1.4 times higher during nighttime supporting the hypothesis that deposited HCHO was degraded especially during daytime when the photochemical activity and hydroxyl radical concentration is higher. Although the samples were collected during daytime and nighttime periods, nighttime samples were exposed to sunlight for 1 to 2 h periods. Probably this caused partial loss of HCHO from nighttime samples and prevented a more pronounced difference between daytime and nighttime samples.

The possibility of loss of deposited HCHO from the WSS by chemical or photochemical degradation was also investigated by spiking experiments. For 55 sampling periods, two WSS samplers were run concurrently one (WSS1) spiked with 150 μg HCHO prior to sampling. Using the deposited amounts ($m_{d1} = m_{d2} = m_d$), spiked amount (m_s) to WSS1, and the measured amounts after sampling (m_1, m_2), fractional loss of deposited HCHO (X_l) can be calculated as:

$$m_1 = (m_s + m_d)\,(1-X_l) \tag{4.22}$$

$$m_2 = m_d\,(1-X_l) \tag{4.23}$$

$$X_l = 1- [(m_1-m_2)/m_s] \tag{4.24}$$

However, calculation of fractional loss is somehow problematic. Because spiking the WSS initially with 150 μg HCHO reduces the fugacity difference and may limit the deposition to WSS1. Since the measured m_1 is biased low, the calculated fractional loss is overestimated (Equation 4.24). Calculations using the temperature adjusted Henry's law constants, gas-phase concentrations and water concentrations indicated that for 11 sampling periods the initial concentration gradient (Equation 4.6) was negative favoring the evaporation of spiked HCHO into the atmosphere. Therefore, the evaluation of spiking experiments should be semi-qualitative rather than quantitative. There was a group of spiked samples (n=19) which their HCHO amounts were lower than the spiked amount and the concentration gradient during sampling was positive, indicating that the loss was not due to evaporation. The loss of the spiked amount for these samples is the lower limit of fractional loss and it ranged between 0.06-0.65 (average=0.32). Since it is overestimated, the average fractional loss calculated using Equation 4.24 can be interpreted as the upper limit value. The average fractional loss calculated from Equation 4.24 was 0.59. Thus, from these results it can be concluded that the actual average fractional loss lies between 0.32 and 0.59.

The results of spiking experiments indicated that the loss of deposited HCHO during field sampling was significant. However, this loss alone can not explain the large difference between modeled and measured mass transfer coefficients in the field experiments. Since none of the mechanisms discussed above (decreased deposition due to non-zero water concentration, sulfite/bisulfite interference, and loss due to chemical degradation or transformation) can fully explain the difference between the modeled and experimental K_g values, the difference was probably due to the propagated effect of these mechanisms.

CHAPTER FIVE
CONCLUSIONS

5.1. Conclusions

Concurrent dry deposition and ambient air samples were collected between May 2003 and May 2004 in Buca, İzmir. Dry deposition of formaldehyde was measured using a water surface sampler (WSS) and dry deposition plates. Wet deposition samples were also collected during the sampling period.

Average gas phase formaldehyde (HCHO) concentrations (7.3±6.5 μg m^{-3}, average± SD) were within the range previously measured at different sites around the world. A six-day sampling program at an urban site indicated that urban concentrations were 4.1 times higher than the suburban concentrations. Daytime and nighttime HCHO concentrations were significantly and positively correlated to the temperature (p<0.01) suggesting that atmospheric HCHO was mainly affected by the photochemical reactions during relatively warmer periods.

Particle phase HCHO concentrations ranged between 3-65 ng m^{-3} (average±SD, 18±12 ng m^{-3}) and HCHO was primarily associated with gas-phase (99.55%). Even though HCHO is a volatile organic compound, the average log K_p (gas/particle partition coefficient, m^3 μg^{-1}) was -4.3±0.5, similar to those observed for semivolatile organic compounds. The octanol-air partition coefficient (K_{OA}) model used to predict the K_p

values for HCHO. However, modeled K_p values were more than five orders of magnitude smaller than the experimental ones. The agreement between experimental K_p values and those predicted for HCHO hydrate was very good, supporting the hypothesis that PM-phase accretion products can revert, during the chemical analysis of the PM to the parent volatile compounds, giving the appearance of anomalously high PM-phase concentrations of parent compounds.

Particle phase HCHO fluxes measured with dry deposition plates ranged between 2-56 μg m^{-2} day^{-1} (average±SD, 17±12 μg m^{-2} day^{-1}). Particulate phase dry deposition velocities for HCHO calculated using the particulate fluxes measured with dry deposition plates and ambient particulate concentrations ranged from 0.1 to 9.6 cm s^{-1} with an average of 1.4±1.4 cm/s. The particulate overall dry deposition velocity agreed well with those measured previously for other pollutants using the same method.

Formaldehyde concentration was measured in 27 rain samples collected at the sampling site ranged between 10-304 μg l^{-1} with an average value of 94±61 μg l^{-1}. The annual formaldehyde wet deposition was calculated as 30155 μg m^{-2} yr^{-1}. The annual HCHO total deposition (wet+dry) was dominated by wet deposition (83.2%).

The range for gas phase HCHO flux was 273-5404 μg m^{-2} day^{-1} and the average value was 1200±888 μg m^{-2} day^{-1}. The average total (gas+particle) flux measured with the WSS was dominated by gas phase flux (98.6%). The calculated K_g values ranged from 0.07 to 0.59 cm s^{-1} with an overall average of 0.25±0.12 cm s^{-1}. The calculated K_g values determined from laboratory experiments ranged from 0.16 to 0.91 cm s^{-1} with an overall average of 0.60±0.22 cm s^{-1}. The average K_g calculated from indoor experiments was 2.4 times higher than the average value calculated from field samples.

The measured K_g values in laboratory were compared to the predictions of the Model I (no enhancement). The statistically significant relationship (r^2=0.50, $p<0.01$) between the measured and modeled K_g indicated that the wind speed is a useful parameter for the

prediction of the mass transfer coefficient in the boundary layer over the WSS. However, the slope of the best-fit model (2.2) indicated that the Model I significantly underestimated the mass transfer coefficient in the boundary layer. The measured K_g values for HCHO were also compared to the predictions of the Model II (chemical enhancement). The statistically significant relationship (r^2=0.59, $p<0.01$) between the measured and modeled K_g, the slope of the regression line (0.98) close to 1.0 and the intercept close to zero indicated an excellent agreement between predicted and measured values. Comparison of overall mass transfer coefficients of formaldehyde predicted by two models and those determined experimentally indicated that under the laboratory conditions of this study, there was a flux enhancement of HCHO mass transfer due to chemical reaction and it ranged between 2.8 and 4.1 (average±SD, 3.6±0.4) times.

For field studies, that there was not a statistically significant linear relationship ($p>0.1$) between the measured and modeled K_g values. The average measured K_g (0.25 cm s^{-1}) was significantly lower than the average predictions of Model I (0.44 cm s^{-1}) and the Model II (0.90 cm s^{-1}). It was suggested that the discrepancy between the mass transfer coefficients measured in the field and those modeled may be due to the following reasons: 1) the assumption of the HCHO concentration in water (C_w) was zero in calculation of K_g does not hold, 2) the interference of sulfite and bisulfite affected the measurement of HCHO in the field samples, 3) losses of deposited HCHO from the WSS by chemical or photochemical degradation. These possible reasons were evaluated by calculations and some additional experiments (i.e., spiking experiments, treatment of the samples for sulfite removal). The results of spiking experiments indicated that the loss of deposited HCHO during field sampling was significant. However, this loss alone could not explain the large difference between modeled and measured mass transfer coefficients in the field experiments. Since none of the proposed mechanisms could fully explain the difference between the modeled and experimental K_g values, the difference was attributed to the propagated effect of these mechanisms.

5.2. Suggestions

Shorter sampling durations should be used for gas-phase deposition to reduce the associated sampling artifacts (i.e., loss of deposited formaldehyde from the water surface sampler). Using a more sensitive analytical method will make possible to use shorter sampling periods. An alternative analytical method is DNPH (2,4-dinitophenylhydrazine) derivatization and HPLC separation and UV detection (Kieber et al., 1999). The detection limit of DNPH derivatization method (0.3 μg l^{-1}) is approximately 25 times lower than the detection limit of the Nash method used in the present study. It will be possible to collect hourly samples using the DNPH method.

The DNPH method is capable to analyze additional aldehydes (acetaldehyde, acroleine, benzaldehyde, butyraldehyde, crotonaldehyde, propionaldehyde) in the same sample. Using this method, the study could be extended to include other aldehydes and their ambient concentrations, gas-particle partitioning, wet and dry deposition, and air-water exchange.

The loss of deposited formaldehyde can be further investigated by analyzing the samples for compounds associated with the reaction of formaldehyde with hydroxyl radical (i.e., formic acid, hydrogen peroxide).

Possible sampling artifacts associated with ambient particle-phase HCHO sampling should be further investigated and quantified. Alternative filter materials like Teflon could be tested to reduce the sampling artifacts.

REFERENCES

Anderson, L.G., Laning, J.A., Barrel, R., Miyagishima, J., Jones, R.H., & Wolfe, P. (1995). Sources and Sinks of Formaldehyde and Acetaldehyde: an Analyses of Denver's Ambient Concentration Data. Atmospheric Environment , 30, 2113-2123.

Andreini, B.P., Baroni, R., Galimbert,i E., & Sesana, G. (2000). Aldehydes in the atmospheric environment: evaluation of human exposure in the north-west area of Milan. Microchical Journal, 67, 11-19.

Báez, A.P., Padilla, H., Cervantes, J., Pereyra, D., Torres, M.C., Garcia, R., &Belmont, R. (2001). Preliminary study of the determination of ambient carbonyls in Xalapa City, Veracruz, Mexico. Atmospheric Environment, 35, 1813-1819.

Báez, A.P., Belmont, R., & Padilla, H. (1994). Measurement of Formaldehyde an Acetaldehyde in the Atmosphere of Mexico City. Environmental Pollution, 89, 163-167.

Barsanti, K.C., & Pankow J.F. (2004). Thermodynamics of the formation of atmospheric organic particulate matter by accretion reactions-Part I: aldehydes and ketones. Atmospheric Environment, 38, 4371-4382.

Betterton, E.A., & Hoffman, M.R. (1988), Henry's Law Constant of Some Environmentally Important Aldehydes. Environmental Science and Technology, 22, 361-367.

Bidleman, T.F. (1988). Atmospheric processes: Wet and dry deposition of organic compounds are controlled by their vapor-particle partitioning. Environmental Science and Technology, 22, 361-367.

Blair, E.W., & Ledbury, W.J. (1925). Partial formaldehyde vapor pressures of aqueous solutions of formaldehyde. J. Chem. Soc., 127, 33-37

Cakan, A. (1999). The direct measurement of the dry deposition of organochlorine pesticides and polychlorinated naphthalenes. Ph.D. Thesis, Illinois Institute of Technology, Chicago, IL.

Cerqueira, M. A., Pio, C. A., Gomes, P. A., Matos, J. S., and. Nunes T. V. (2003). Volatile organic compounds in rural atmospheres of central Portugal. The Science of The total Environment, 313, 49-60.

Chénier, R. (2003), An Ecological Risk Assessment of Formaldehyde. Human and Ecological Risk Assessment 9, 483-509.

Ching, S.W., Barry, S.E., & Zaromb, S. (1998). Detection and Estimation of Part-per-Billion Levels of Formaldehyde Using a Portable High-Throughput Liquid Absorption Air Sampler. Environmental Science and Technology, 32, 169-176.

Christensen, C.S., Skov, H., Nielsen, T., & Lohse, C. (2000). Temporal variation of carbonyl compound concentrations at a semi-rural site in Denmark. Atmospheric Environment, 34, 287-298.

Deandrade, J.B., Pinheiro, H.L.C., & Andrade M.V. (1993). Determination of Formaldehyde and Acetaldehyde Associated to Atmospheric Aerosols by HPLC. International Journal of Environmental Analytical Chemistry, 52, 49-56.

Deandrade, J.B., Pinheiro H.L.C., & Andrade M.V. (1995). The Formaldehyde and Acetaldehyde Content of Atmospheric Aerosol. Journal of The Brazilian Chemical Society, 6 , 287-290.

Dong, S., Dasgupta, P.K. (1986). Solubility of gaseous formaldehyde in liquid water and generation of trace standard gaseous formaldehyde. Environmental Science and Technology, 20, 637–640.

Economou, C., & Mihalopoulos N. (2002). Formaldehyde in the rainwater in the eastern Mediterranean: occurrence, deposition and contribution to organic carbon budget, Atmospheric Environment, 36, 1337-1347.

Environment Canada (1999a). Canadian Environmental Protection Act, Priority Substances List, Supporting document for the environmental assessment of formaldehyde. Hull, Quebec, Environment Canada, Commercial Chemicals Evaluation Branch.

Fierro, I.V., Popp, C.J., & Martin, R.S. (2004). Biogenic emissions and ambient concentrations of hydrocarbons, carbonyl compounds and organic acids from ponderosa pine and cottonwood trees at rural and forested sites in Central New Mexico. Atmospheric Environment, 38, 249-260.

Finlayson-Pitts, B. J. & Pitts, Jr. J.N. (1986). Atmospheric Chemistry, Fundamentals and Experimental Techniques, John Wiley & Sons, New York.

Franz, T.P., Eisenreich, S.J., & Holsen T.M. (1998). Dry deposition of particulate polychlorinated biphenyls and polycyclic aromatic hydrocarbons to Lake Michigan., Environmental Science and Technology, 32, 3681-3688.

Gallagher, M.W., Beswick, K.M., Duyzer, J., Westrate, H., Choularton, T.W. & Hummelshoj, P. (1997). Measurements of aerosol fluxes to speulder forest using a micrometeorological technique. Atmospheric Environment, 31, 359-373.

Granby, K., Christensen, C.S., Lohsen, C. (1997). Urban and semi-rural observations of carboxylic acids and carbonyls. Atmospheric Environment, 31, 1403-1415.

Grosjean, E., Grosjean, D., Seinfeld, J.H. (1996a). Atmospheric chemistry of 1-octene, 1-decene cyclohexene: gas-phase carbonyl and peroxyacyl nitrate products. Environmental Science and Technology, 30, 1038–1047.

Grosjean, E., de Andrade, J.B., Grosjean, D. (1996b). Carbonyl products of the gas-phase reaction of ozone with simple alkenes. Environmental Science and Technology, 30, 975–983.

Halsall, C.J., Coleman P.J., Davis, B.J., Burnett, V., Waterhouse, K.S., Harding-Jones, P., & Jones, K.C. (1994). Polycyclic aromatic hydrocarbons in U.K. urban air. Environmental Science and Technology, 28, 2380-2386.

Harner, T., & Bidleman, T.F. (1998). Octanol-air partition coefficient for describing particle/gas partitioning of aromatic compounds in urban air. Environmental Science and Technology, 32, 1494-1502.

Ho, K.F., Lee, S.C., Louie, P.K.K and Zou, S.C. (2002). Seasonal variation of carbonyl compound concentrations in urban area of Hong Kong. Atmospheric Envitonment, 36, 1259-1265.

Hoff, R.M., Strachan, W.M.J., Sweet, C.W., Chan, C.H., Shackleton, M., Bidleman, T.F., Brice, K.A., Burniston, D.A., Cussion, S., Gatz, D.F., Harlin, K., & Schroeder, W.H. (1996). Atmospheric deposition of toxic chemicals to the Great Lakes: A review of data through 1994. Atmospheric Environment, 30, 3505-3527.

Holsen, T.M., Noll, K.E., Liu, S.P., and Lee, W.J. (1991). Dry deposition of polychlorinated biphenyls in urban areas. Environmental Science and Technology, 25, 1075-1081.

Holsen, T.M., Noll, K.E. (1992). Dry deposition of atmospheric particles: application of current models to ambient data. Environmental Science and Technology, 26, 1807-1815.

Hsu, Y-K. (1997). MS Thesis, Illinois Institute of Technology, Chicago, IL.

Jang, M., and Kamens, R.M. (2001). Characterization of secondary aerosol from the photooxidation of toluene in the presence of NO_x and 1-Propene. Environmental Science and Technology, 35, 3626-3639.

Kamens, R.M., & Jaoui, M. (2001). Modeling aerosol formation from α-pinene+NO_x in the presence of natural sunlight using gas-phase kinetics and gas-particle partitioning theory. Environmental Science and Technology, 35, 1394-1405.

Kaupp, H., & McLahlan, M.S. (1999). Atmospheric particle size distributions of polychlorinated dibenzo-p-dioxins and dibenzofurans (PCDD/Fs) and polycyclic aromatic hydrocarbons (PAHs) and their implications for wet and dry deposition. Atmospheric Environment, 33, 85-95.

Kawamura, K., Steinberg, S., Ng L., & Kaplan I.R. (2001). Wet deposition of low molecular weight mono-and di-carboxylic acids, aldehydes and inorganic species in Los Angeles. Atmospheric Environment, 35, 3917-3926.

Kesselmeier, J., Bode, K., Hofmann, U., Müller, H., Schafer, L., Wolf, A., Ciccioli, P., Brancaleoni, E., Cecinato, A., Frattoni, M., Foster, P., Ferrari, C., Jacob, V., Fugit, J. L., Dutaur, L., Simon, V., and Torres, L. (1997). Emission Of Short Chained Organic Acids, Aldehydes And Monoterpenes From Quercus I.Lex L. and Pinus Pinea L. In Relation To Physiological Activities, Carbon Budget And Emission Algorithms. Atmospheric Environment Volume, 31, SI, 119-133.

Kesselmeier, J., Kuhn, U., Wolf, A., Andreae, M. O., Ciccioli, P., Brancaleoni, E., Frattoni, M., Guenther, A., Greenberg, J., De Castro Vasconcellos, Telles de Oliva, P., Tavares, T. and Artaxo, P. (2000). Atmospheric volatile organic compounds (VOC) at a remote tropical forest site in central Amazonia. Atmospheric Environment, 34, 4063-4072.

Khare, P., Satsangi, G.S., Kumar, N., Maharajkumari, K., & Srivastava, S. S. (1997). HCHO, HCOOH and CH3COOH in Air and Rain Water at a Rural Tropical Site in North Central India. Atmospheric Environment, 31, 3867-3875.

Khwaja, H.A. (1995). Atmospheric concentrations of carboxylic acids and related compounds at a semiurban site. Atmospheric Environment, 29, 127-139.

Kieber R.J., Rhines M.F., Willey J.D., & Brooks A.Jr.G. (1999). Rainwater formaldehyde: concentration, deposition and photochemical formation. Atmospheric Environment, 33, 3659-3667.

Kieber, R.J., Zhou, X., Mopper, K. (1990). Formation of carbonyl compounds from UV-induced photodegradation of humic substances in natural waters: Fate of riverine carbon in the sea. Limnology and Oceanography, 35,1503–1515.

Kim, E., Kalman, D., & Larson, T. (2000). Dry deposition of large airborne particles onto a surrogate surface. Atmospheric Environment, 34, 2387-2397.

Kim, B.R., Kalis, E.M., DeWulf, T., Andrews, K.M. (2000). Henry's law constants for paint solvents and their implications on volatile organic compound emissions from automotive painting. Water Environment Research, 72, 65-74.

Klippel, W., & Warneck, P. (1980). The formaldehyde content of the atmospheric aerosol. Atmospheric Environment, 14, 809-818.

Largiuni, O., Giacomelli, M. C. & Piccardi G. (2002). Concentration of Peroxides and Formaldehyde in Air and Rain and Gas-Rain Partitioning. Journal of Atmospheric Chemistry, 41, 1–20.

Lee, B. K., & Lee, C. B. (2004). Development Of An Improved Dry And Wet Deposition Collector And The Atmospheric Deposition Of PAHs Onto Ulsan Bay, Korea. Atmospheric Environment, 38, 863–871.

Liggio, J., & McLaren, R. (2003). An Optimized Method For The Determination Of Volatile And Semi-Volatile Aldehydes and Ketons In Ambient Particulate Matter. International Journal of Environmental Analytical Chemistry, 83, 819-835.

Lyman, W.J., Reehl, W.F., & Rosenblatt, D.H. (1990). Handbook of Chemical Property Estimation Methods, Environmental Behavior of Organic Compounds. American Chemical Society, Washington DC.

Mackay, D., & Yeun, A.T.K. (1983). Mass transfer coefficient correlations for volatilization of organic solutes from water. Environmental Science and Technology, 17, 211-217.

Morales, J.A., Bifano C. & Escalona A. (1998). Atmospheric deposition of SO_4-S and (NH_4 + NO_3)-N at two rural sites in the Western Maracaibo lake basin, Venezuela. Atmospheric Environment, 32, 3051-3058.

Nuccio, J., Seaton, P.J., & Kieber, R.J. (1995). Biological production of formaldehyde in the marine environment, Limnology and Oceanography, 40, 521–527.

NIOSH Manual of Analytical Methods (NMAM), Fourth Edition, (1994). Method 3500.

Odabasi, M. (1998). The measurement of PAH dry deposition and air-water exchange with the water surface sampler. PhD thesis, Illinois Institute of Technology.

Odabasi, M., Sofuoglu, A., Vardar, N., Tasdemir Y., & Holsen TM. (1999). Measurement of dry deposition and air-water exchange of polycyclic aromatic hydrocarbons with the water surface sampler. Environmental Science and Technology, 33, 426-434.

Odabasi, M., Sofuoglu, A., & Holsen, T. M. (2001). Mass Transfer Coefficients for Polycyclic Aromatic Hydrocarbons (PAHs) to the Water Surface Sampler: Comparison to modeled results. Atmospheric Environment, 35, 1655-1662.

Odabasi, M., & Bagiroz, H.O. (2002). Sulfate Dry Deposition Fluxes and Overall Deposition Velocities Measured with a Surrogate Surface. The Science of the Total Environment, 297, 193-201.

Odabasi, M., Muezzinoglu, A., Bozlaker, A. (2002). Ambient Concentrations and Dry Deposition Fluxes of Trace Elements in Izmir, Turkey. Atmospheric Environment, 36, 5841-5851.

Odabasi, M., Sofuoglu, A., Vardar, N., Tasdemir, Y. and Holsen, T.M. (1999). Measurement of dry deposition and air-water exchange of polycyclic aromatic hydrocarbons with the water surface sampler. Environmental Science and Technology, 33, 426-434.

Park, J. S., Wade, T. L., Sweet, S. T. (2002). Atmospheric deposition of PAHs, PCBs, and organochlorine pesticides to Corpus Christi Bay, Texas. Atmospheric Environment, 36, 1707–1720.

Pena, R.M., Garcia, S., Herrero, C., Losada, M., Vazquez, A., & Lucas T. (2002). Organic acids and aldehydes in rainwater in a northwest region of Spain. Atmospheric Environment, 36, 5277-5288.

Possanzini, M., Di Palo, V., & Cecinato A. (2002). Sources and photodecomposition of formaldehyde and acetaldehyde in Rome ambient air. Atmospheric Environment, 36, 3195-3201.

Sakugawa, H., & Kaplan, I. R. (1993). Measurements of H_2O_2, aldehydes and organic acids in Los Angeles rainwater: their sources and deposition rates. Atmospheric Environment, 27B, 203-219.

Sanhueza E., Ferrer Z., Romero J., & Santana M. (1991). HCHO and HCOOH in tropical rains. Ambio 20, 115-118.

Satsumabayashi, H, Kurita, H, Chang, YS, Carmichael, GR, & Ueda H. (1995). Photochemical formations of lower aldehydes and lower fatty acids under long-range transport in central Japan. Atmospheric Environment, 29, 255–266.

Schwarzenbach, R.P., Gschwend, P.M. & Imboden, D.M. (1993). Environmental Organic Chemistry, Wiley-Interscience, New York.

Schwarzenbach, R. P, Gschwend, P. M, & Imboden, D.M. (2003). Environmental Organic Chemistry 2nd Edition, Wiley-Interscience, New York.

Seinfeld, J. H. (1986). Atmospheric Chemistry and Physics of Air Pollution, John Wiley and Sons, New York.

Shahin, U., Lu, J, Yi, S.M, Paode, R.D., & Holsen T.M. (2000). Long-term elemental dry deposition fluxes measured around Lake Michigan with an automated dry deposition sampler. Environmental Science and Technology, 34, 1887-1892.

Shahin, U. M., Holsen, T.M. & Odabasi, M. (2002). Dry Deposition Measured with a Water Surface Sampler: A Comparison to Modeled Results. Atmospheric Environment, 36, 3267-3276.

Shahin, U.M., Zhu, X., & Holsen, T.M. (1999a.), Dry deposition of reduced and reactive nitrogen: a surrogate surface approach. Environmental Science and Technology, 33, 2113-2117.

Shoeib, M., Harner, T. (2002). Using measured octanol-air partition coefficients to explain environmental partitioning of organochlorine pesticides. Environmental Toxicology and Chemistry, 21, 984-990.

Sofuoglu, A., Cetin, E., Bozacioglu, S.S., Sener, G.D., and Odabasi, M. (2004). Short-term variation in ambient concentrations and gas/particle partitioning of organochlorine pesticides in Izmir, Turkey. Atmospheric Environment, 38, 4483-4493.

Tanner, P.A., Law, P.T., & Tam, W.F. (2001). Comparison of aerosol and dry deposition sampled at two sites in Southern China. Journal of Aerosol Science, 32, 461-472.

Tasdemir, Y. (1997). Modification and evaluation of a water surface sampler to investigate the dry deposition and air-water exchange of polychlorinated biphenyls (PCBs). Ph.D. Thesis, Illinois Institute of Technology, Chicago, IL.

Tasdemir, Y., Odabasi, M., Vardar, N., Sofuoglu, A., Murphy, J.T., & Holsen T.M. (2004). Dry deposition fluxes and velocities of polyclorinated biphenyls (PCBs) associated with particles. Atmospheric Environment, 38, 2447-2456.

Tobias, H.J., & Ziemann, P.J. (2000). Thermal desorption mass spectrometric analysis of organic aerosol formed from reactions of 1-Tetradecene and O3 in the presence of alcohols and carboxylic acids. Environmental Science and Technology, 34, 2105-2115.

US EPA (1993). Motor vehicle-related air toxics study. Ann Arbor, MI, US Environmental Protection Agency, Office of Mobile Sources, Emission Planning and Strategies Division, (EPA 420-R-93-005).

U.S. Consumer Product Safety Commission (1997). An Update on Formaldehyde. (CPSC)(U.S. EPA) Revision.

Xiao, H., and Wania, F. (2003). Is vapor pressure or the octanol–air partition coefficient a better descriptor of the partitioning between gas phase and organic matter? Atmospheric Environment, 37, 2867-2878.

Vardar, N., Odabasi, M., and Holsen, T.M. (2002). Particulate Dry Deposition and Overall Deposition Velocities of Polycyclic Aromatic Hydrocarbons (PAHs). Journal of Environmental Engineering, 128, 269-274.

Vardar, N., Tasdemir, Y., Odabasi, M., & Noll K.E. (2004). Characterization of atmospheric concentrations and partitioning of PAHs in the Chicago atmosphere. Science of The Total Environment, 327, 163-174.

Viskari, E.L., Vartiainen, M. & Pasanen, P. (2000). Seasonal and diurnal variation in formaldehyde and acetaldehyde concentrations along a highway in Eastern Finland, Atmospheric Environment, 34, 917-923.

Winkelman, J.G.M., Ottens, M., Beenackers, A.A.C.M. (2000). The kinetics of dehydration of methylene glycol. Chemical Engineering Science, 55, 2065-2071.

Winkelman, J.G.M., Voorwinde, O.K., Ottens, M., Beenackers, A.A.C.M., Jansen L.P.B.M. (2002). Kinetics and chemical equilibrium of the hydration of formaldehyde, Chemical Engineering Science, 57, 4067-4076.

WEB_1. (2002). World Health Organization Concise International Chemical Assessment Document 40**,**

http://www.inchem.org/documents/cicads/cicads/cicad40.htm, 05/01/2004.

WEB_2. (2002). The effect of UV-radiation on photo-oxidants and formaldehyde in the atmosphere Riedel, K., Weller, R., Schrems, O., http://www.niwa.co.nz/rc/atmos/uvconference/Riedel.pdf, (03/05/2004)

WEB_3. (2004). Virtual Computational Chemistry Laboratory (VCCL), http://146.107.217.178/lab/alogps/start.html, 20/07/2004.

Wyers, G.P. & Duyzer, J.H. (1997). Micrometeorological measurement of dry deposition flux of sulphate and nitrate aerosols to coniferous forest. Atmospheric Environment, 31, 333-343.

Yi, S-M., Holsen, T.M., & Noll, K.E. (1997). Comparison of dry deposition predicted from models and measured with a water surface sampler. Environmental Science and Technology, 31, 272-278.

Yi, S-M., Shahin, U., Sivadechathep, J., Sofuoglu, S.C., & Holsen, T.M. (2001). Overall elemental dry deposition velocities measured around Lake Michigan. Atmospheric Environment, 35, 1133-1140.

Zeller, K, Donev, E, Bojinov, H & Nikolov, N. (1997). Air pollution status of the Bulgarian Govedartsi ecosystem, Environmental Pollution 98. 281-289.

Zhang, L., Gong, S., Padro, J., Barrie, L., (2001). A size-segregated particle dry deposition scheme for an atmospheric aerosol module. Atmospheric Environment, 35, 549-560.

Zhou, X., Mopper, K. (1997). Photochemical production of low-molecular-weight carbonyl compounds in seawater and surface micro layer and their air-sea exchange, Marine Chemistry, 56, 201-213.